

II International Workshop on Simulations of HIC for NICA Energies
JINR (Dubna), April 16-18, 2018

**Study of dynamics of heavy-ion collisions
at NICA:
EoS, directed and elliptic flow, freeze-out
and femtoscopy correlations**

SINP MSU: G. Eyyubova, I. Lokhtin, L. Malinina (also in JINR),
S. Sivoklov, A. Snigirev

UiO: L. Bravina, E. Zabrodin

Outlook

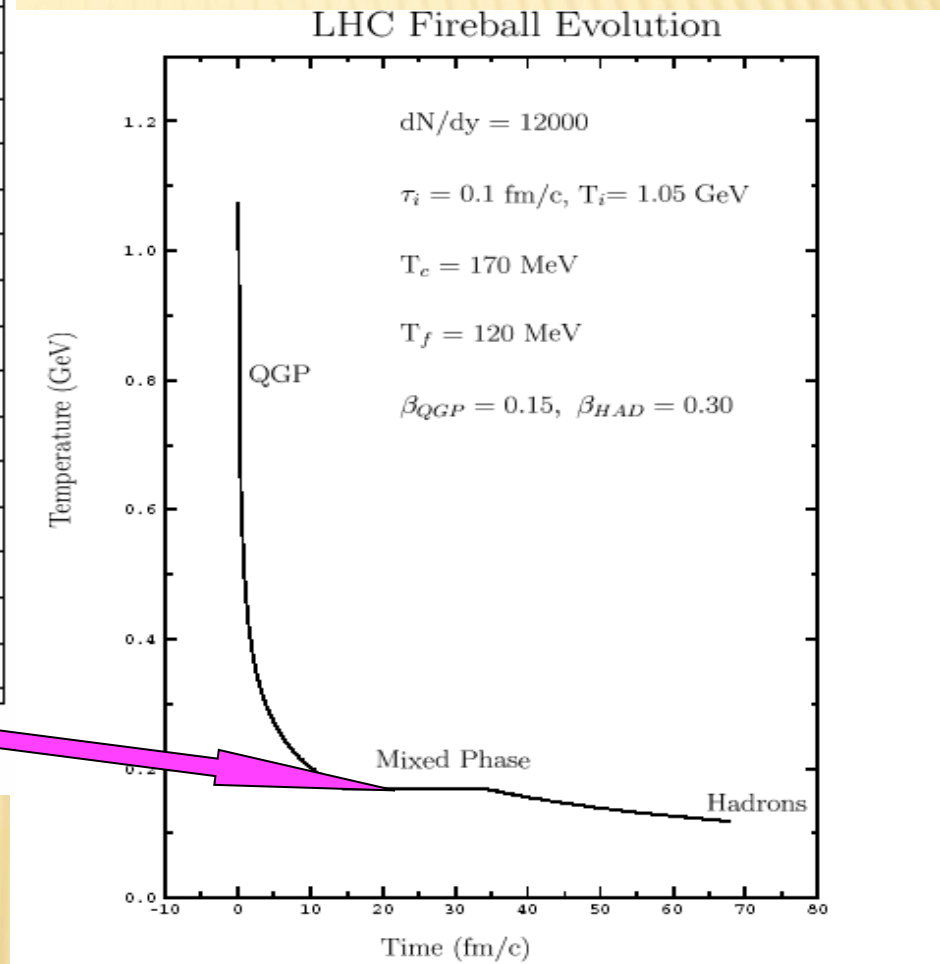
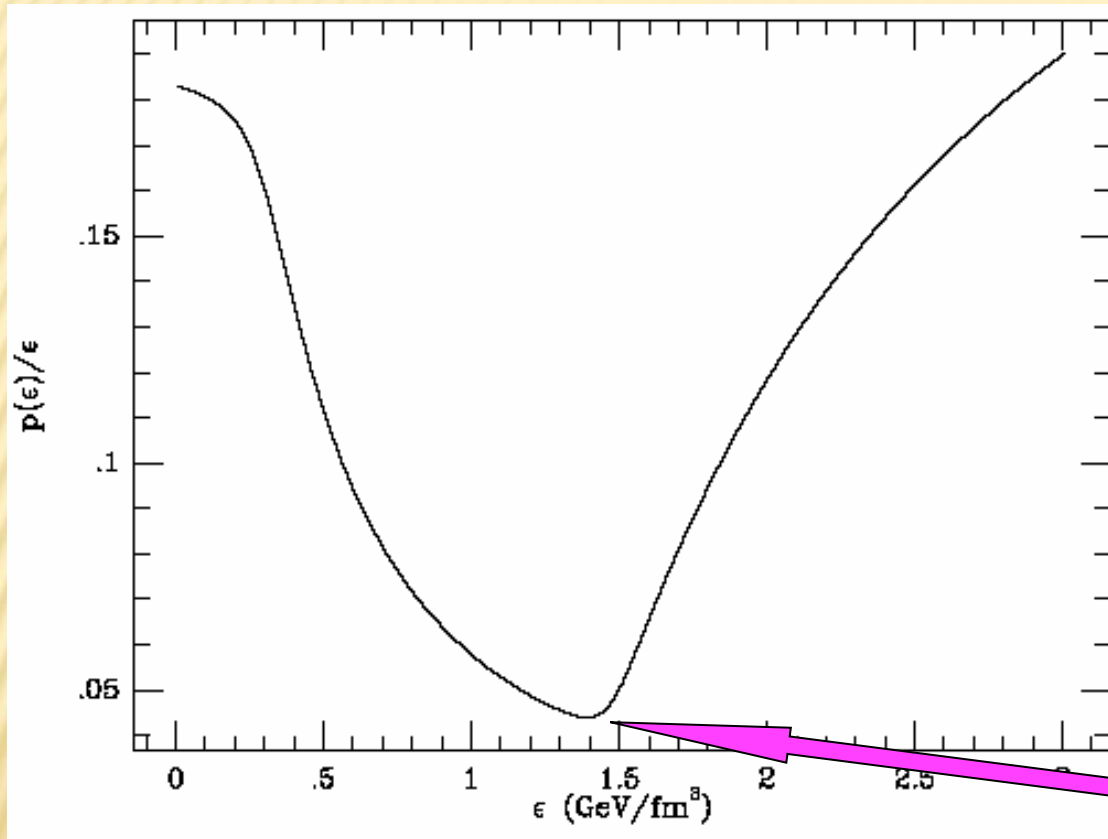
- **Investigation of flow effects and freeze-out dynamics in heavy-ion (HI) collisions at NICA energies.**
- **Study of femtosopic observables in HI collisions at NICA energies.**
- **Investigation of the relaxation of quark-hadron matter to the equilibrium state in microscopic models. Extraction of equation of state (EoS) of hot and dense nuclear matter produced in HI collisions at NICA energies.**

1. Flow and freeze-out

in collaboration with

Yu. Kvasiuk, A. Oshlyanskyi, D. Sachenko and S. Vityuk

DISAPPEARANCE OF DIRECTED FLOW



Hung and Shuryak, PRL 75 (1995) 4003

Braun-Munzinger, NPA 661 (1999) 261c

In case of first order phase transition

$$\frac{dP}{d\epsilon} = c_s^2 = 0$$

DIR.FLOW OF NUCLEONS AND FRAGMENTS AT LOWER ENERGIES

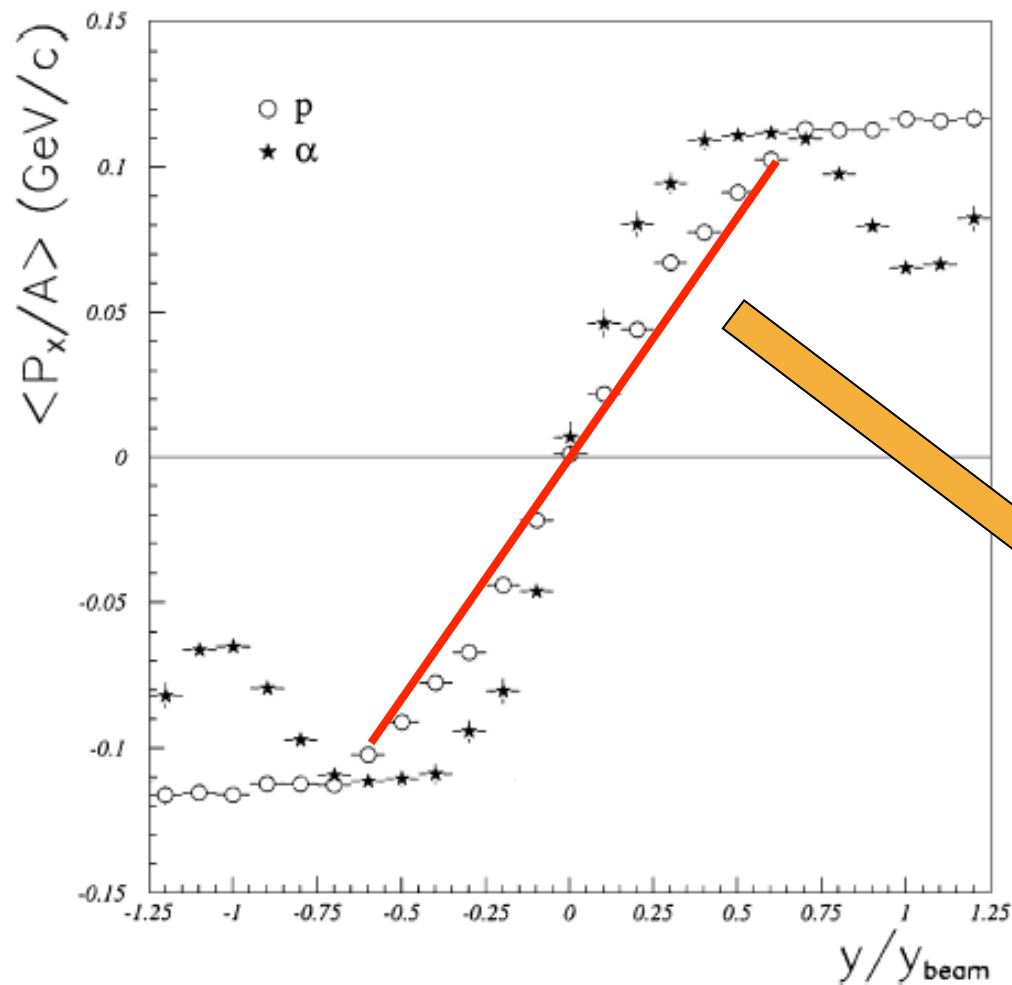


Figure 1 Average in-plane transverse momentum versus normalized rapidity in the reaction Au+Au at 800.4 MeV. The points at $y/y_{\text{beam}} < 0$ are reflected.

Plastic Ball Collaboration
introduced a slope parameter

$$F = \frac{d\langle p_x \rangle / A}{dy_n}, \quad y_n = y / y_{\text{max}}$$

$$F_y = \frac{d\langle p_x \rangle / A}{dy}$$

**Directed flow of nucleons
and fragments has linear
slope in normal direction
=> normal flow**

W. Reisdorf, H.G. Ritter
Annu.Rev.Nucl.Part.Sci. 47 (1997) 663

SOFTENING OF DIRECTED FLOW

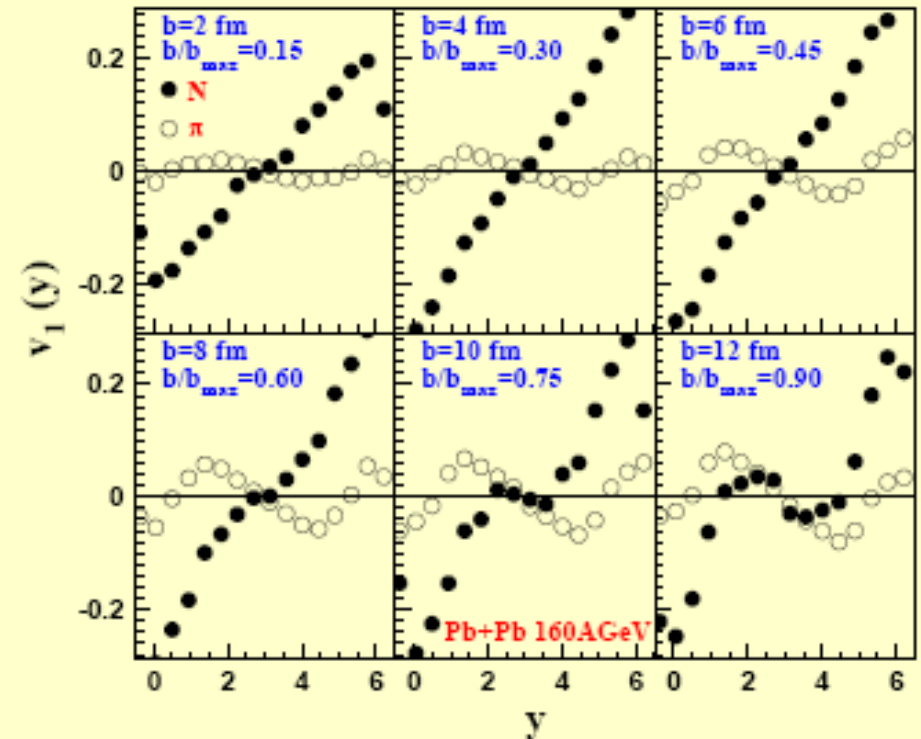
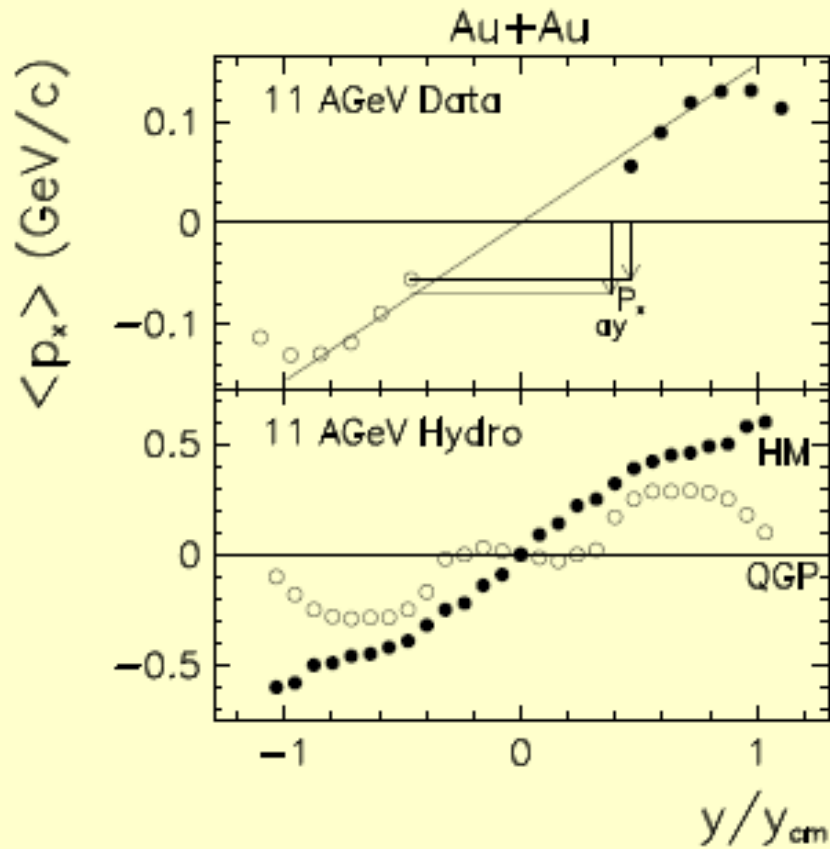
L.P. Csernai, D. Röhrich, PLB 458 (1999) 454

L. Bravina, PLB 334, 49 (1995)

H. Liu, S. Panitkin, N. Xu, PRC 59, 348 (1999)

R.J.M. Snellings *et al.*, PRL 84, 2803 (2000)

L. Bravina *et al.*, PRC 61, 064902 (2000)



Transition to the **Quark-Gluon Plasma**
 → decrease in pressure → softening
 of the directed flow

Wiggle structure: The effect is more pronounced in peripheral and light-ion collisions, therefore, it cannot be explained by the softening of the **EOS** because of the formation of strings

Beam energy scan results for v_1 (STAR)

S. Singha et al. (STAR Collab.), PoS CPOD2017 (2018) 004

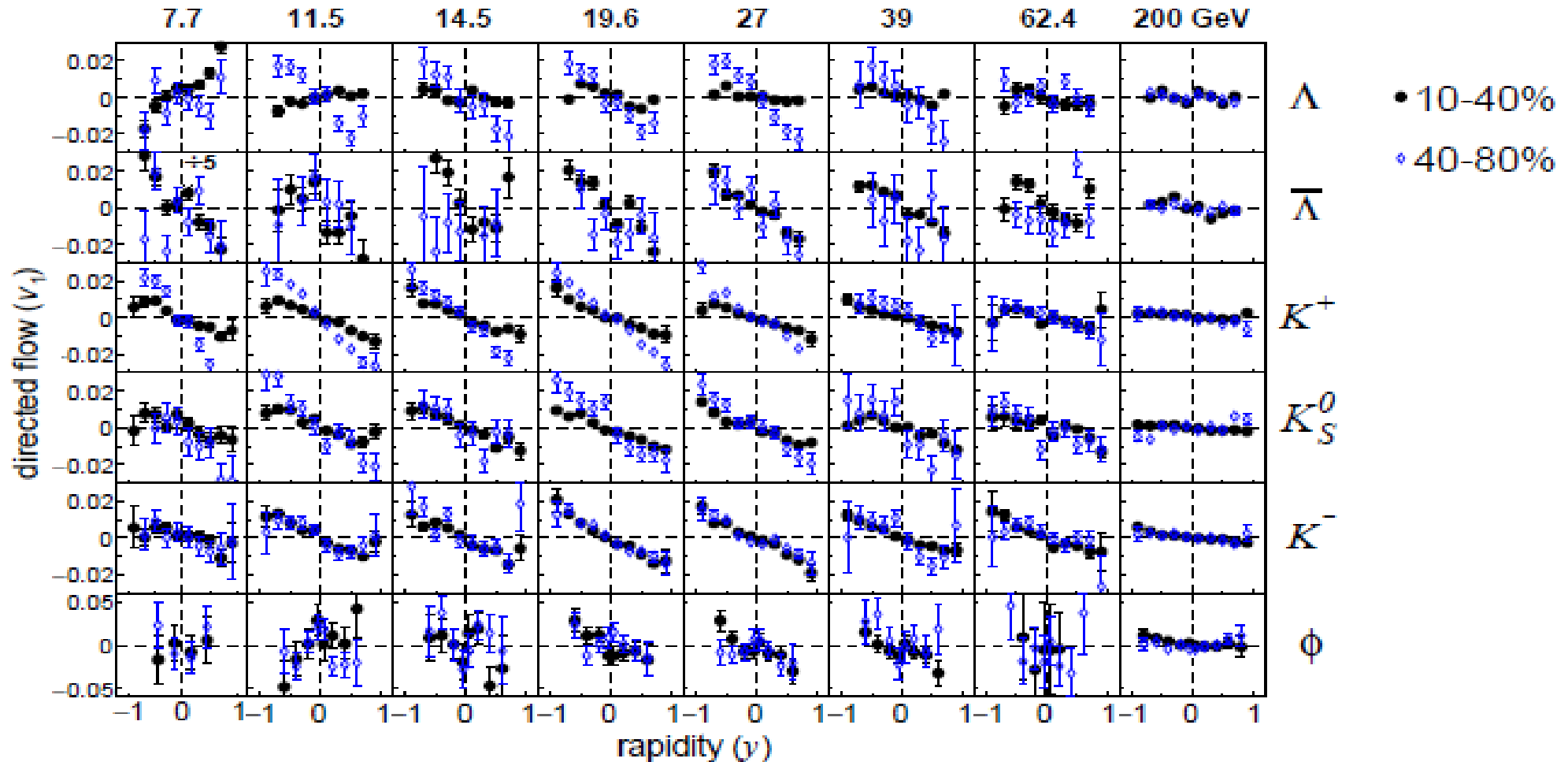
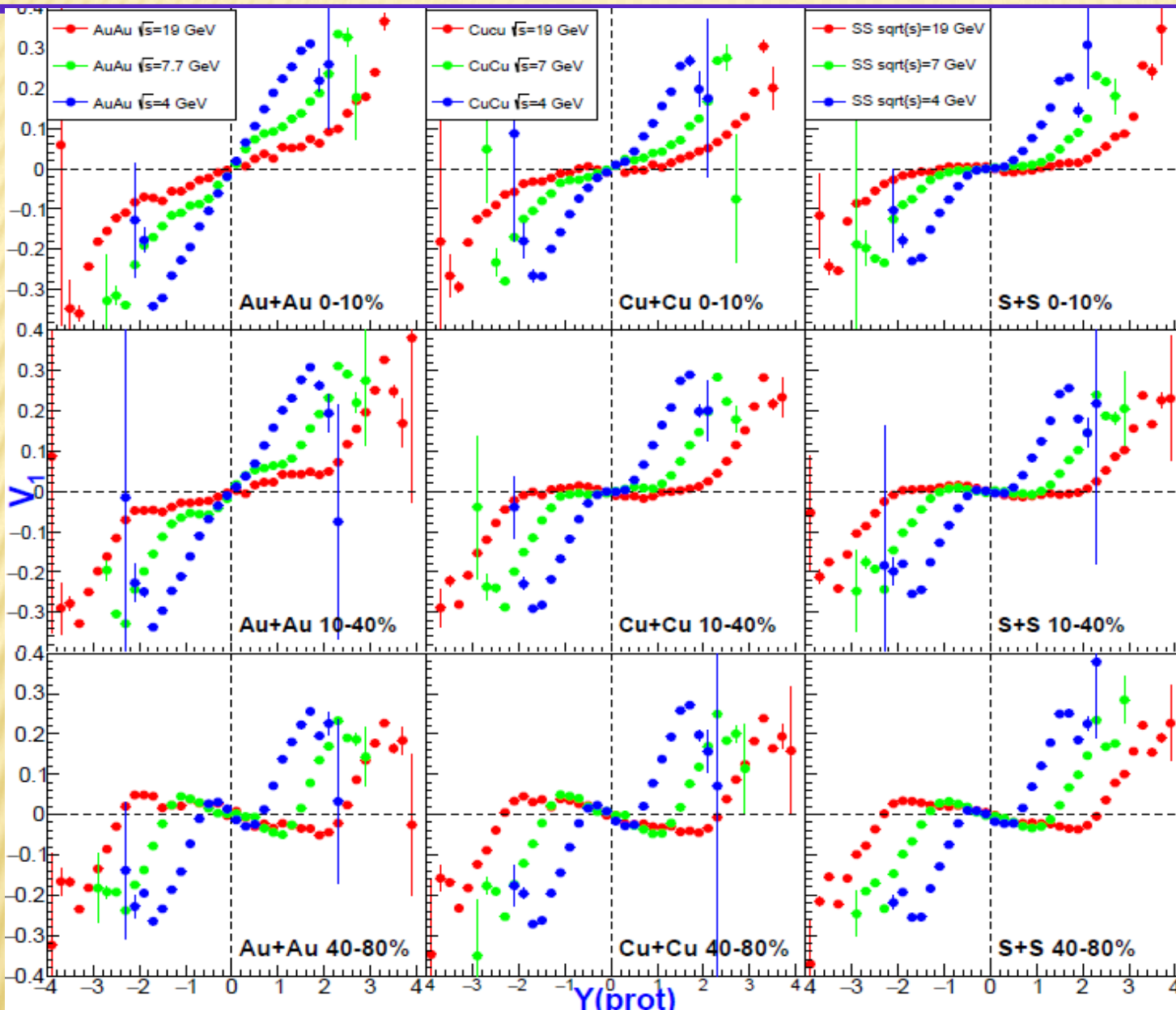


Figure 1: (Color online) Rapidity dependence of directed flow (v_1) for Λ , $\bar{\Lambda}$, K^+ , K_S^0 , K^- and ϕ in 10-40% and 40-80% Au+Au collisions at $\sqrt{s_{NN}} = 7.7, 11.5, 14.5, 19.6, 27, 39, 62.4$ and 200 GeV.

Directed flow of protons in light and heavy systems



QGSM

Blue - $\sqrt{s} = 4 \text{ GeV}$
 Green - 7.7 GeV
 Red - 19 GeV

- Softening and development of antiflow at midrapidity with increasing impact parameter
- In central events – “normal” flow with decreasing CM energy
- Softening of v_1 at midrapidity is stronger for small colliding systems, whereas in case of QGP formation the effect should be opposite

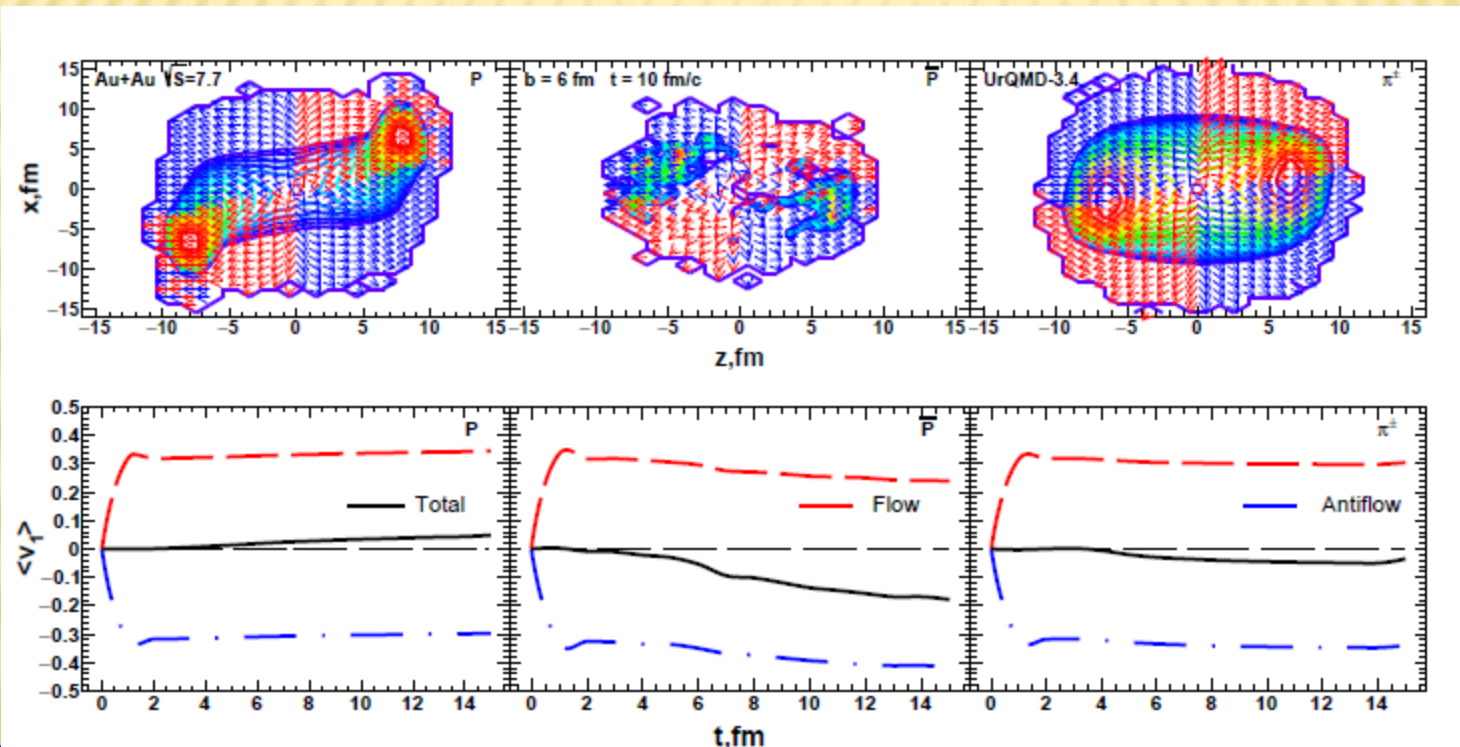
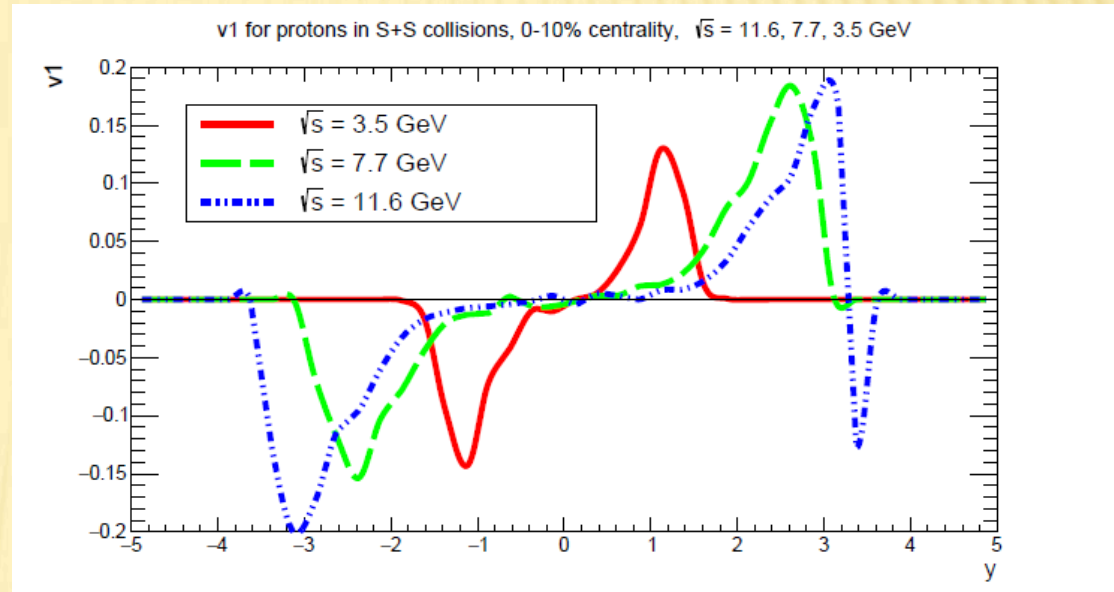
Au + Au

Cu + Cu

S + S

Directed flow in HI collisions at NICA energies

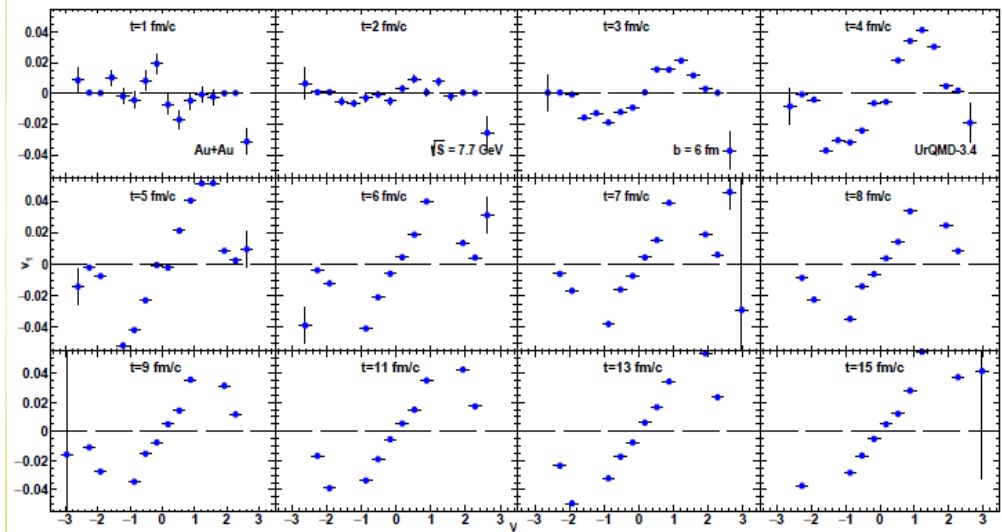
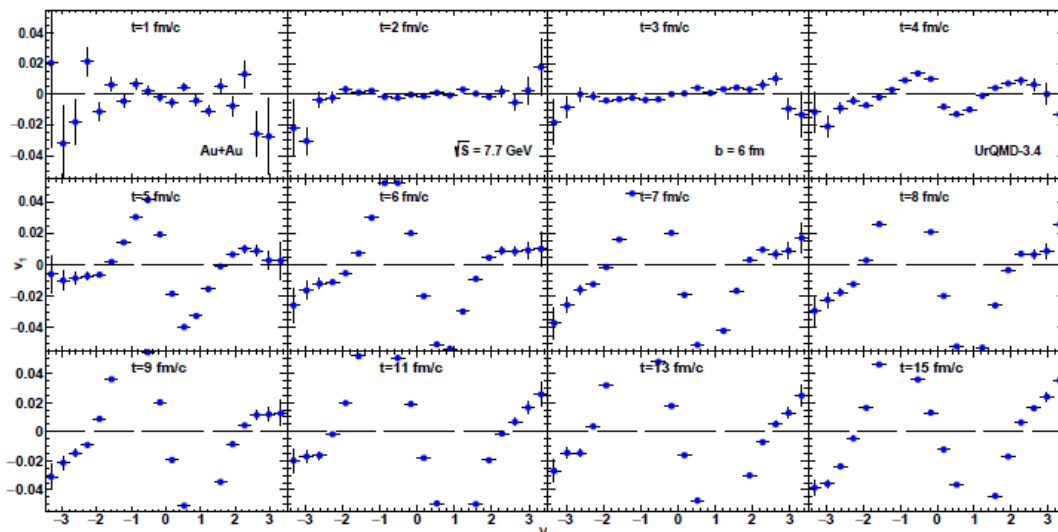
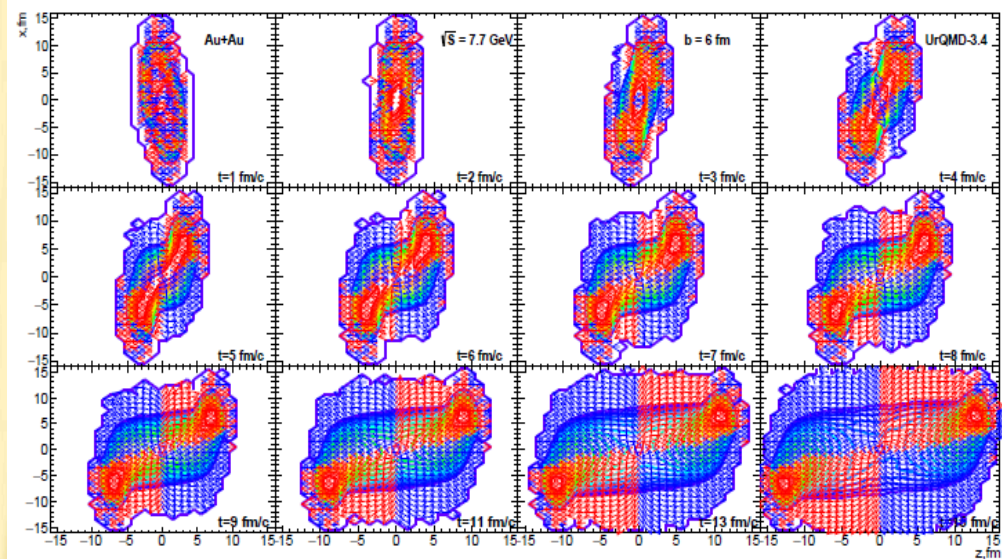
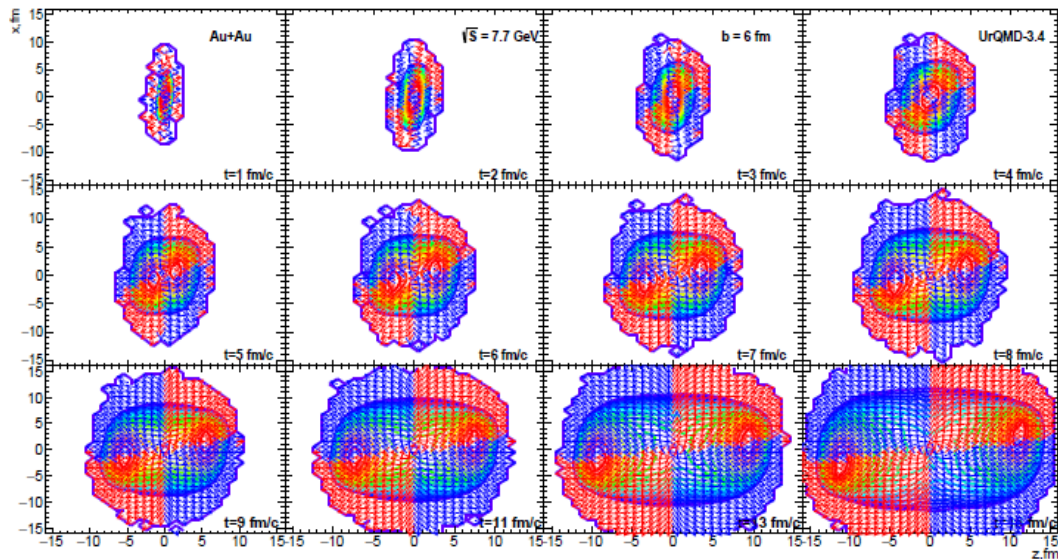
Origin of changing of proton directed flow from antiflow to normal flow with decrease of CM energy in microscopic transport models:
 Spectator peaks which demonstrate normal flow behavior become closer to each other



UrQMD calculations

- Directed flow = Normal flow – Antiflow

Time development of directed flow



pions

Au+Au @ 7.7 GeV

b = 6 fm

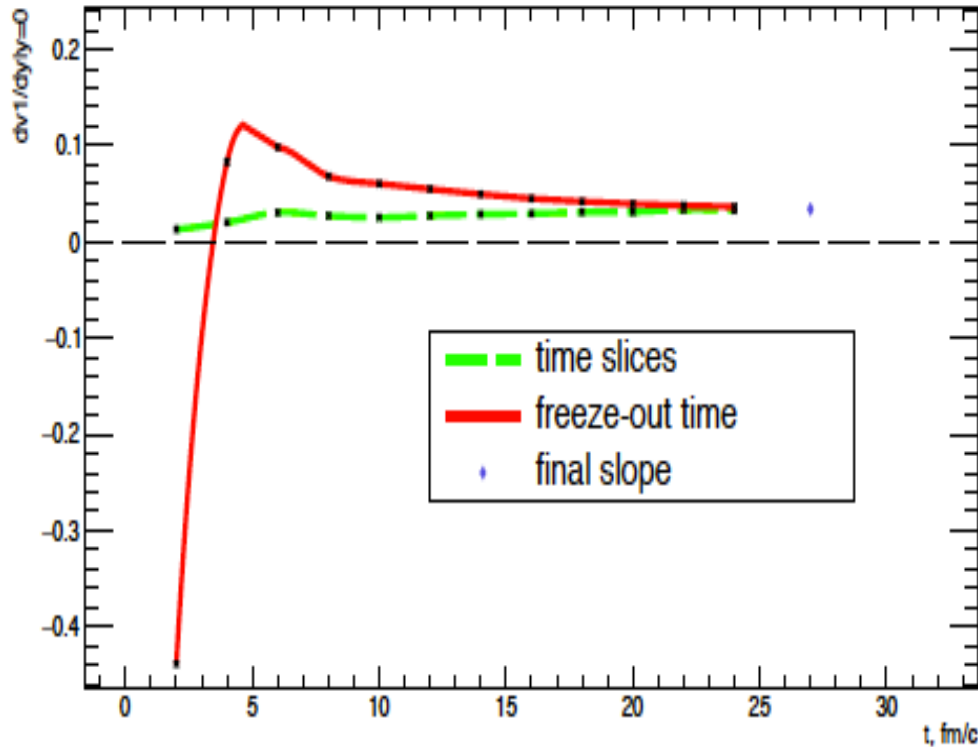
protons

● V_1 of both pions and protons at midrapidity is formed at approximately 7 – 12 fm/c

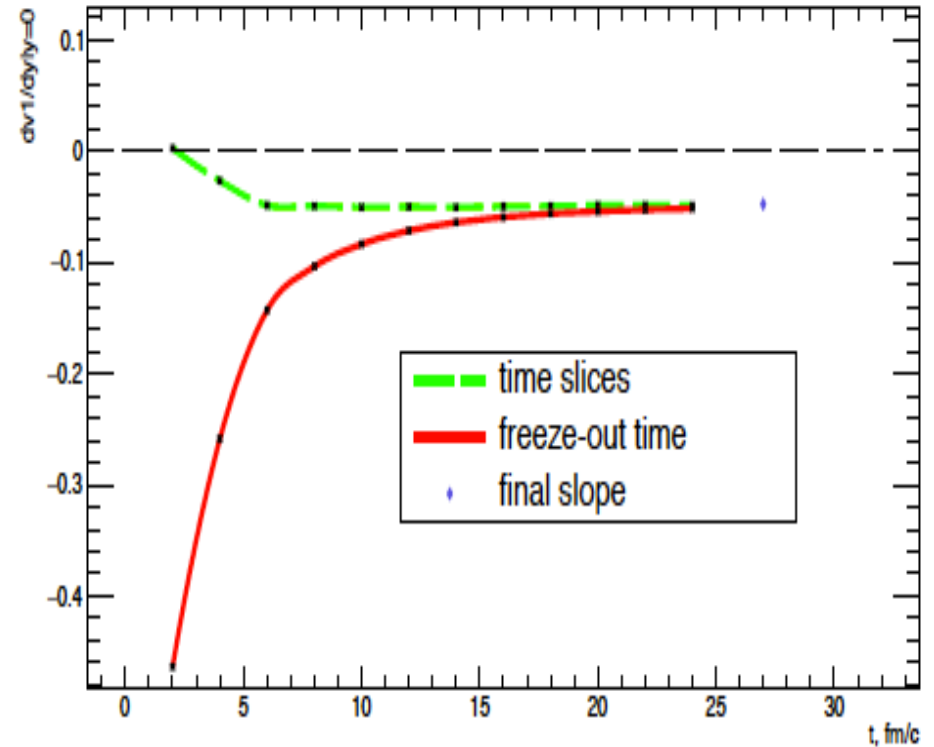
Time evolution of directed flow at NICA energies

$$dv_1/dy (y=0)$$

Protons, Au+Au, $\sqrt{s}=11.6$, $b=6$



Pions, Au+Au, $\sqrt{s}=11.6$, $b=6$



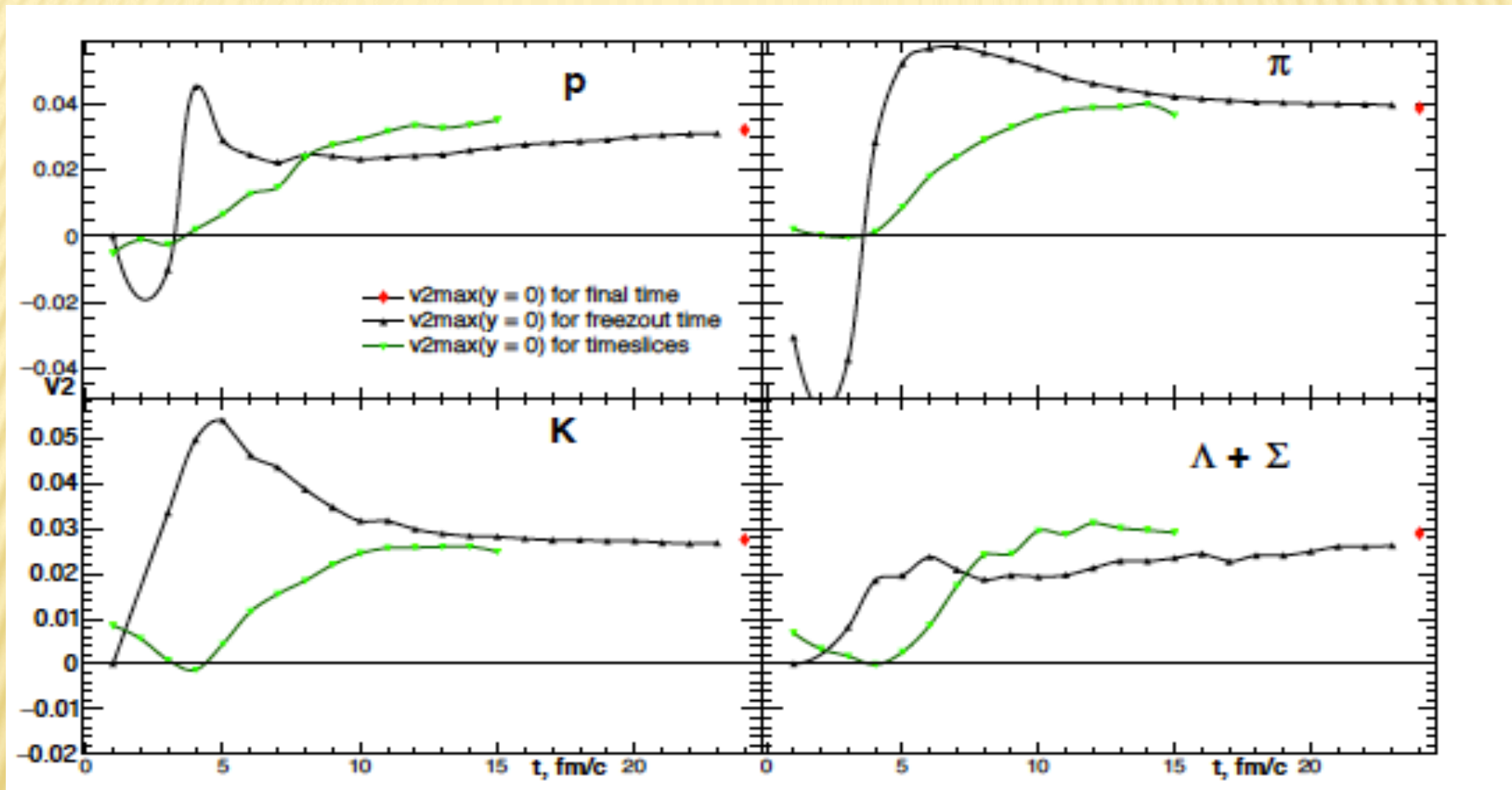
protons

pions

Directed flow at midrapidity is developing until $t = 10$ fm/c

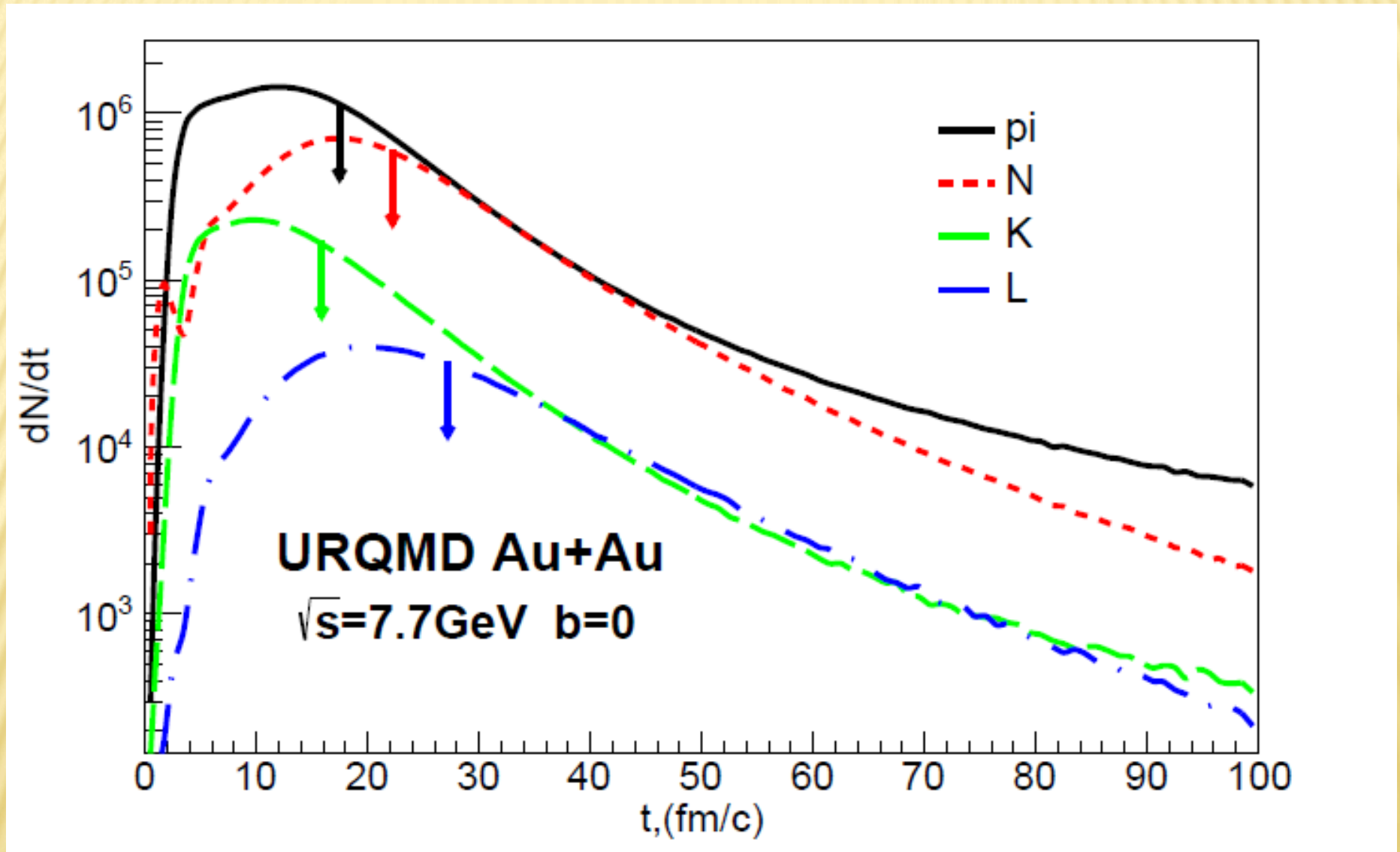
Time evolution of elliptic flow at NICA energies

Au+Au @ 7.7 GeV ; b=6fm



- Negative v_2 of pions and protons frozen at first 3 fm/c
- Protons, pions, kaons frozen between 3 and 10 fm/c carry stronger elliptic flow
- v_2 is developing until $t = 12$ fm/c or later => we need to investigate freeze-out

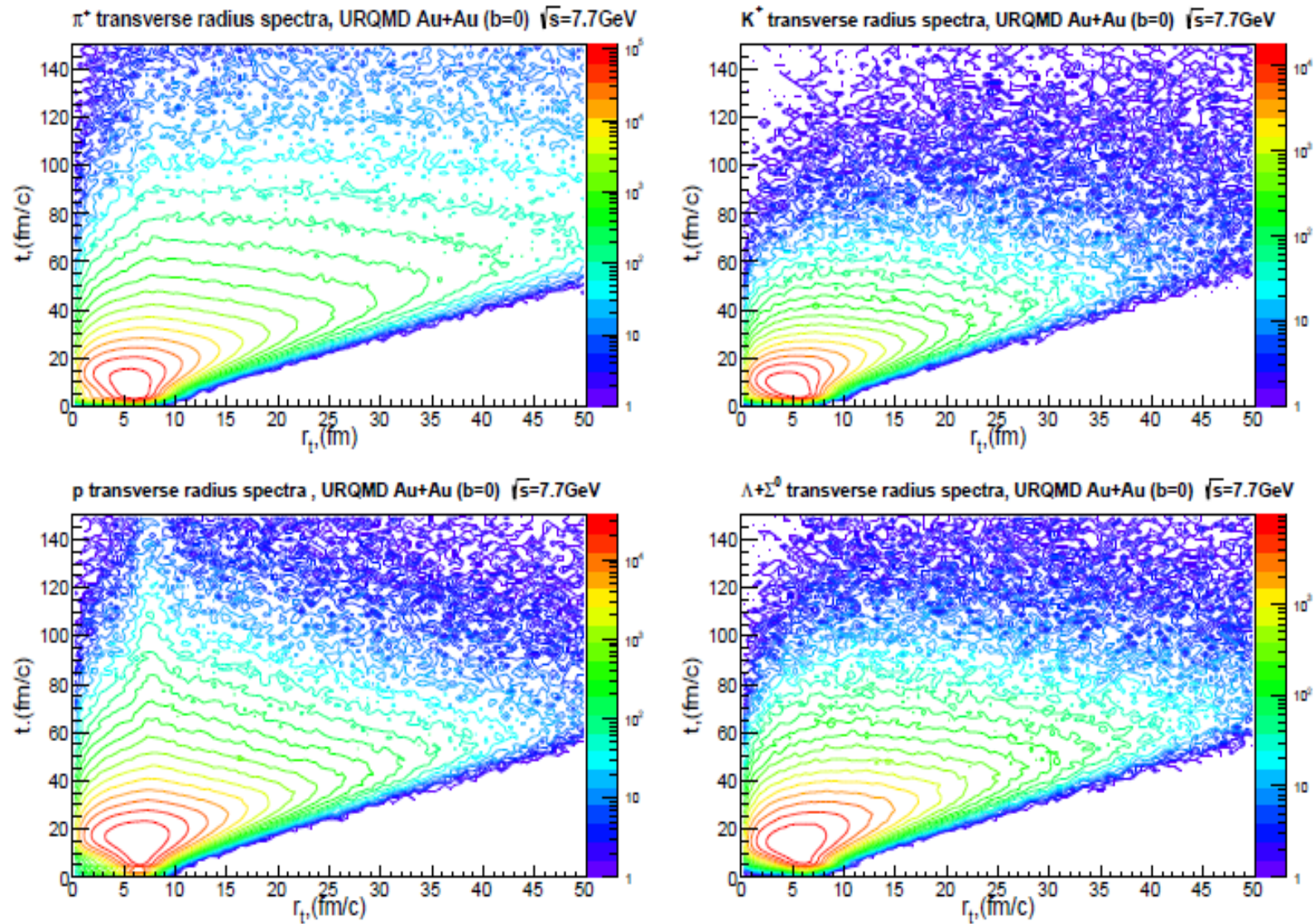
Sequential freeze-out of hadrons at NICA energies



- There is no sharp freeze-out for different hadrons
- The order of freeze-out is as follows: mesons (kaons and pions), nucleons and lambdas

Freeze-out of hadrons at NICA energies

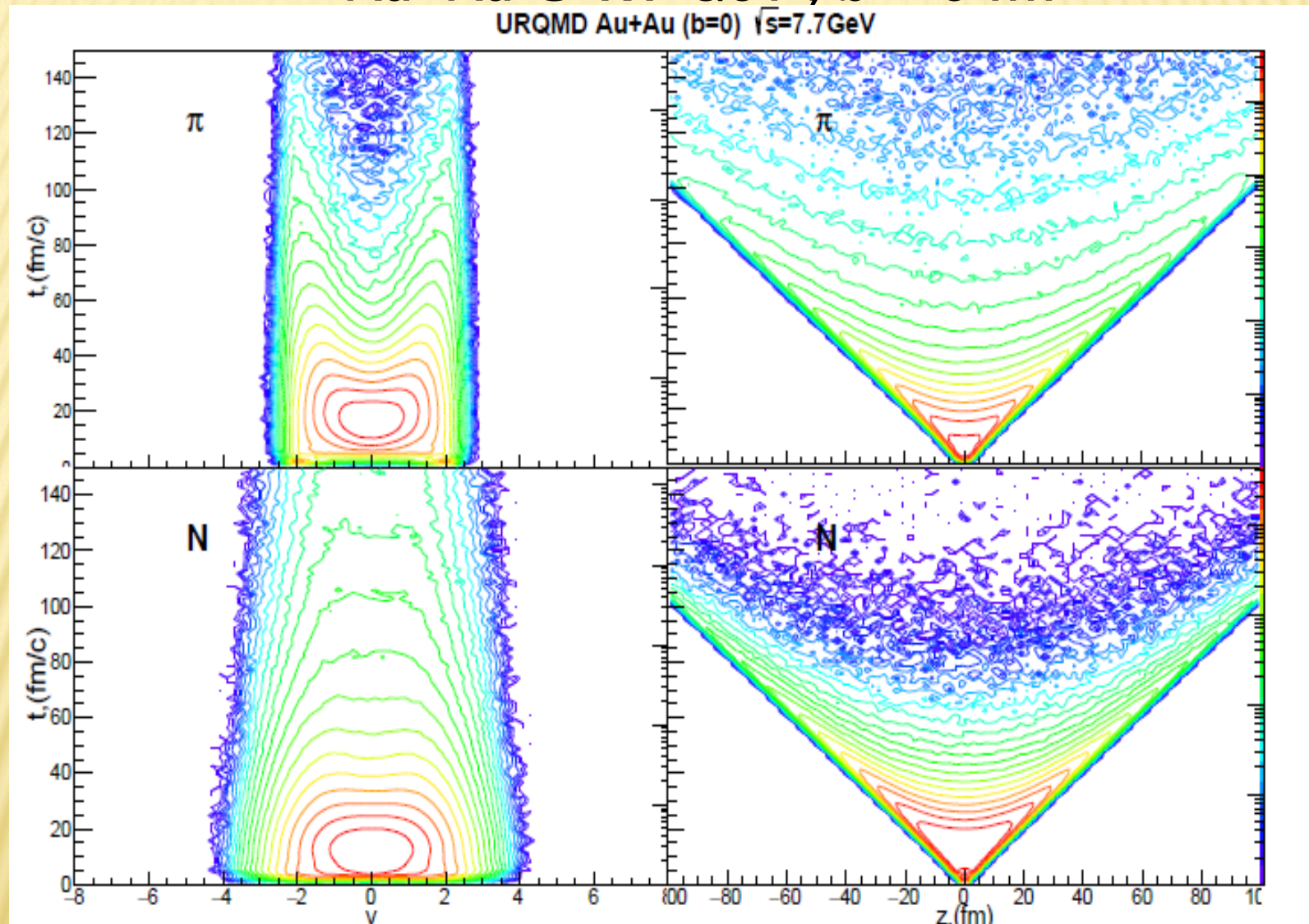
Au+Au @ 7.7 GeV ; $b = 0$ fm



● Baryons are emitted longer and from larger areas than mesons

Freeze-out of hadrons at NICA energies

Au+Au @ 7.7 GeV ; $b = 0$ fm



● Baryons are emitted longer and from larger areas than mesons

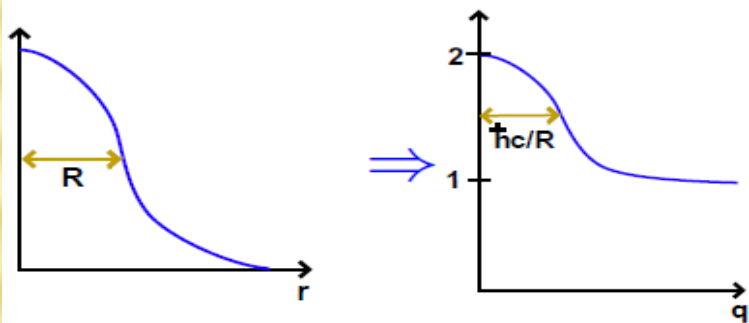
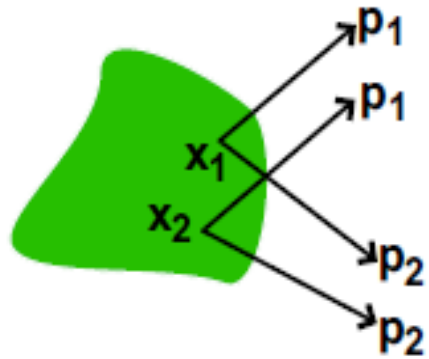
Summary of flow and freeze-out studies for NICA

- **Directed flow = Normal flow – Antiflow**
- **Softening of directed flow can be misinterpreted as the softening of the EOS due to QGP formation, but:
QGP => the effect is stronger for heavy nuclei (Au+Au or Pb+Pb)
Cascade => the effect is stronger for light colliding systems**
- **v_1 development at midrapidity takes about 15 fm/c**
- **Different species decouple at different times. The order of the hadronic freeze-out is as follows:
1-2 - pions and kaons, 3 – nucleons, 4 - lambdas**

2. Correlation femtoscopy

Correlation Femtoscopy

Correlation femtoscopy : measurement of space-time characteristics $R, c\tau \sim \text{fm}$ of particle production using particle correlations due to the effects of quantum statistics (**QS**) and final state interactions (**FSI**)



- **Two particle Correlation Function (CF):**

- **Theory:**
$$C(q) = \frac{N_2(p_1, p_2)}{N_1(p_1) \cdot N_2(p_1)}, C(\infty) = 1$$

- **Experiment:**
$$C(q) = \frac{S(q)}{B(q)}, q = p_1 - p_2$$

$S(q)$ – pairs from same event

$B(q)$ – pairs from different event

- **Parametrization:**

- **1D:**
$$C(q_{inv}) = 1 + \lambda \exp(-R^2 q_{inv}^2)$$
 , R Gaussian radius in Pair Rest Frame (**PRF**), λ correlation strength parameter

- **3D:**
$$C(q_{out}, q_{side}, q_{long}) = 1 + \lambda \exp(-R_{out}^2 q_{out}^2 - R_{side}^2 q_{side}^2 - R_{long}^2 q_{long}^2)$$

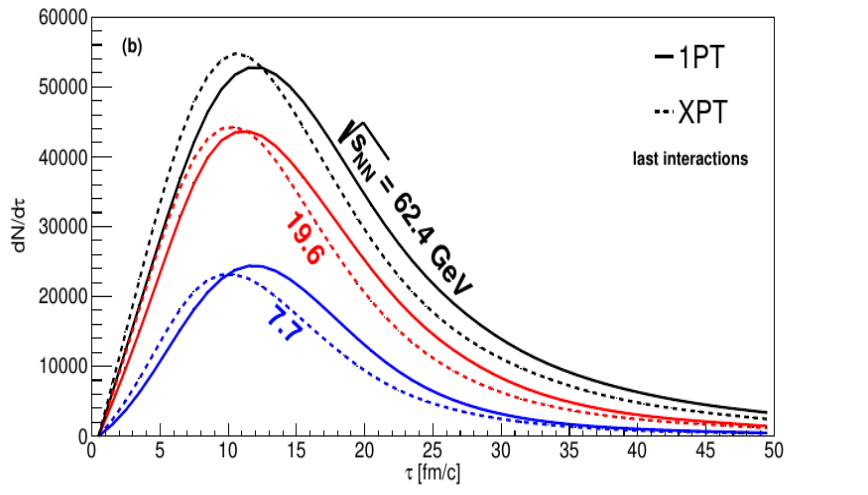
where both R and q are in Longitudinally Co-Moving Frame (**LCMS**)
 long || beam; out || transverse pair velocity v_T ; side normal to out, long

Study of phase transition with femtoscopy

STAR, Phys.Rev. C92 (2015) 1, 014904

Emission times for 1st order phase transition are larger than for crossover.

Pion emission times at the last interactions



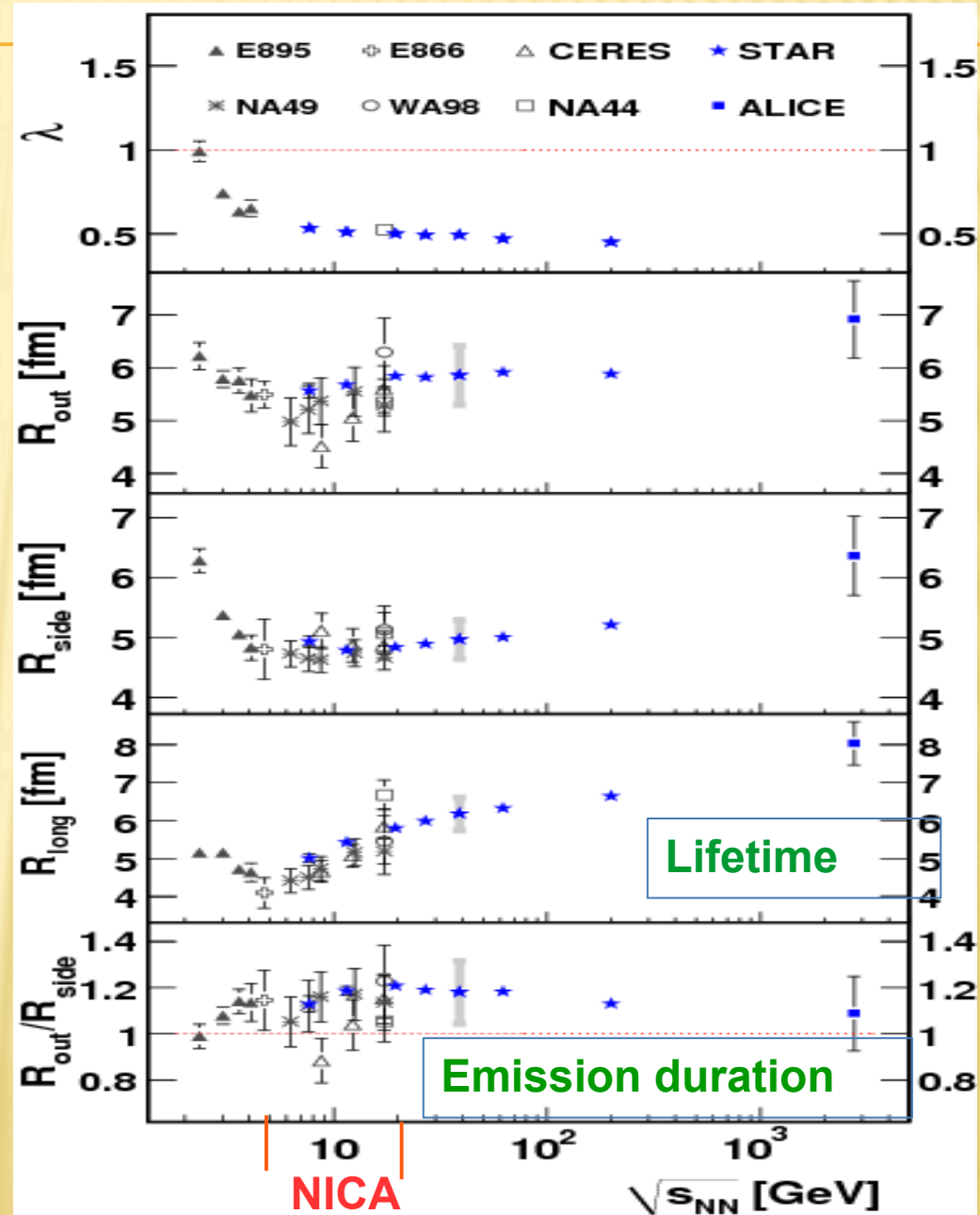
We study the possibilities to extract this difference experimentally at the MPD using femtoscopy technique

“Correlation femtoscopy study at energies available at the JINR Nuclotron-based Ion Collider Facility and the BNL Relativistic Heavy Ion Collider within a viscous hydrodynamic plus cascade model”,

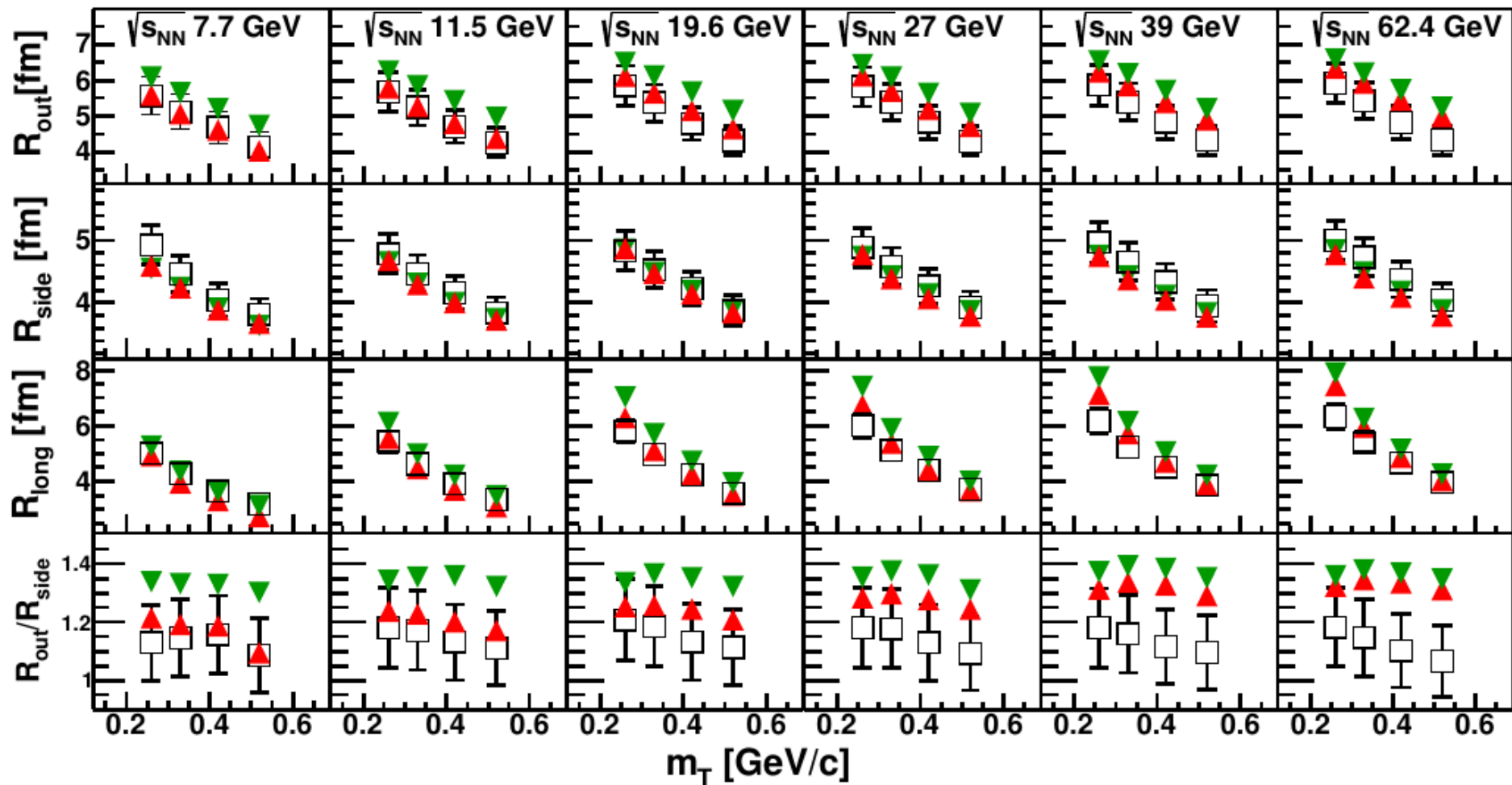
Phys.Rev. C96 (2017) no.2, 024911

P. Batyuk, Iu. Karpenko, R. Lednicky, L. Malinina,

K. Mikhaylov, O. Rogachevsky, D. Wielanek)



3D Pion radii versus m_T with vHLLE+UrQMD model



Green triangles - 1PT EoS, **Red triangles** - XPT EoS, **Open black squares** STAR data BES

- R_{out} (XPT) at high energies and R_{out} (1PT) at all energies are slightly overestimated -> an indication of the need to reduce the emission time in the model
- $R(1PT) > R(XPT)$ by ~ 1 fm for “out” and “long” radii

Source functions

The new Source Function technique was tested.

SF for 1st order is wider than the one for crossover.

Main advantage of this technique is the possibility to use the Source Functions itself without any hypothesis about its shape.

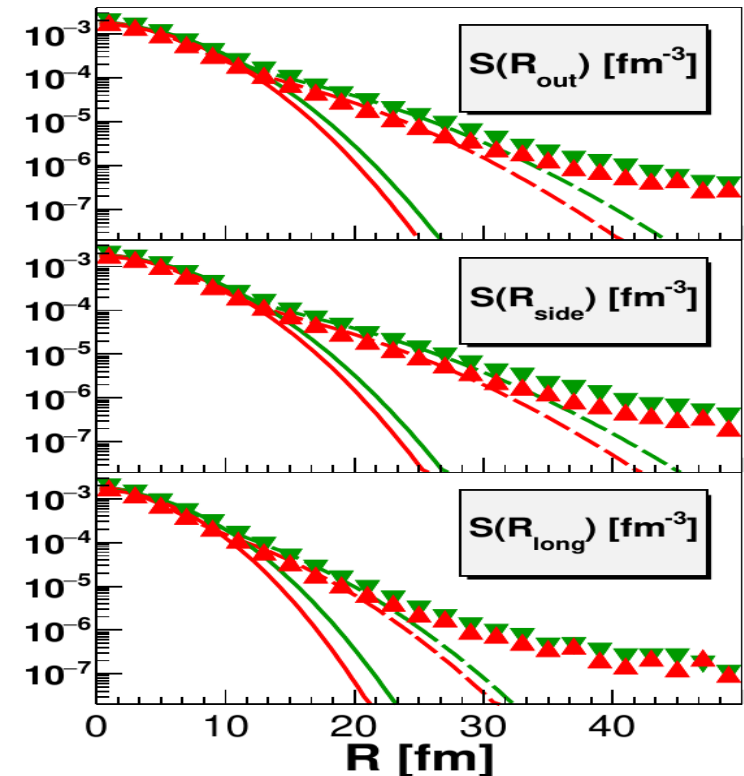
$$C(\mathbf{k}^*, \mathbf{P}) = \int d^3\mathbf{r}^* S^\alpha(\mathbf{r}^*, \mathbf{P}) \left| \psi_{-\mathbf{k}^*}^{S, \alpha' \alpha}(\mathbf{r}^*) \right|^2,$$

Different functions were tested to describe the shape of SF projections: single Gaussian

$$S(\vec{r}^*) \sim \exp\left(-\frac{r_{out}^{*2}}{4R_{out}^{*2}} - \frac{r_{side}^{*2}}{4R_{side}^{*2}} - \frac{r_{long}^{*2}}{4R_{long}^{*2}}\right),$$

$$S^H(r_x, r_y, r_z) = \lambda \exp\left[-f_s\left(\frac{x^2}{4r_{xs}^2} + \frac{y^2}{4r_{ys}^2} + \frac{z^2}{4r_{zs}^2}\right) - f_l\left(\frac{x^2}{4r_{xl}^2} + \frac{y^2}{4r_{yl}^2} + \frac{z^2}{4r_{zl}^2}\right)\right],$$

$$f_s = 1/[1 + (r/r_0)^2], \quad f_l = 1 - f_s.$$



Gaussian + Gaussian;
Gaussian + Lorencian
Gaussian + Exp

Hump-function

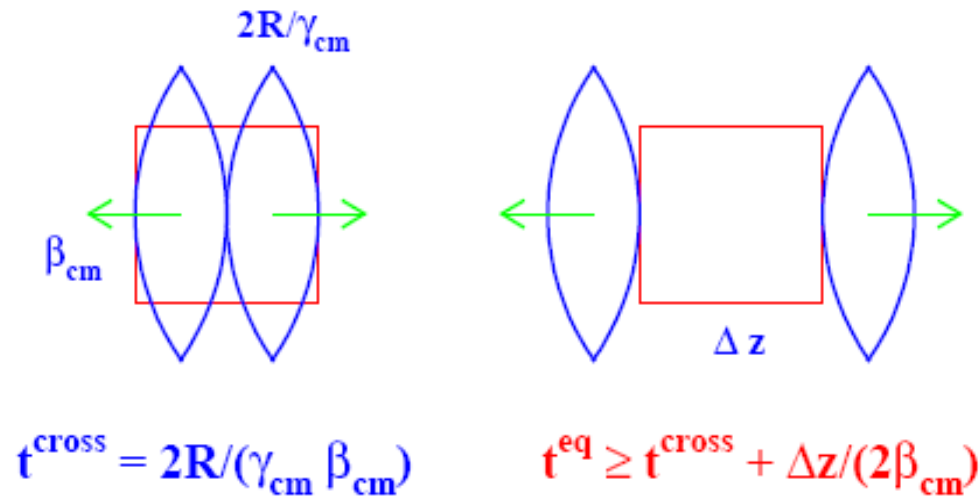
- The best description was obtained with Gaussian+Gaussian and Hump-function.
- Gaussian+Gaussian - simple interpretation (core-resonances) & more stable fitting procedure

Summary of pion femtoscopy studies for NICA

- Possibility to distinguish between hybrid model source functions with 1st order phase transition and crossover was studied using vHLLE+UrQMD model
 - Hydro phase lasts longer with 1st order PT.
 - Hadronic cascade diminishes the difference between 1PT and XPT source functions, though there is still a possibility to distinguish them using the femtoscopy technique.
 - vHLLE+UrQMD model with XPT describes RHIC femtoscopy radii at $\sqrt{s} = 7.7-62.4$ GeV
 - There is an indication that optimal description of the femtoscopy radii requires about 1 fm shorter pion emission time with the present setup of the model, at all collision energies. – new tune of vHLLE+UrQMD model is needed.
 - It'll be very interesting to try to use 3 phase hydro model (THESEUS) at low energies
 - $R_{out}(1PT) > R_{out}(XPT)$ & $R_{long}(1PT) > R_{long}(XPT)$
-
- Source functions technique allows to get an additional information about differences between 1PT / XPT; Best parametrizations of SF : Gauss+Gauss and Hump
 - The standard one-Gaussian parametrization of the 3D CF reflects correctly the behaviour of the SF at small r^* and is sufficiently sensitive to EoS.
 - It is very promising to make 3D CF analysis using heavier particles: K,p because of more Gaussian shape of SF and less influence of resonances

3. Relaxation to equilibrium and Equation of State (EOS)

EQUILIBRATION IN THE CENTRAL CELL



Kinetic equilibrium:

Isotropy of velocity distributions
 Isotropy of pressure

Thermal equilibrium: Energy spectra of particles are described by Boltzmann distribution

$$\frac{dN_i}{4\pi p E dE} = \frac{V g_i}{(2\pi\hbar)^3} \exp\left(\frac{\mu_i}{T}\right) \exp\left(-\frac{E_i}{T}\right)$$

Chemical equilibrium:

Particle yields are reproduced by SM with the same values of

$$(T, \mu_B, \mu_S):$$

$$N_i = \frac{V g_i}{2\pi^2 \hbar^3} \int_0^\infty p^2 dp \exp\left(\frac{\mu_i}{T}\right) \exp\left(-\frac{E_i}{T}\right)$$

STATISTICAL MODEL OF IDEAL HADRON GAS

input values

output values

$$\epsilon^{\text{mic}} = \frac{1}{V} \sum_i E_i^{\text{SM}}(T, \mu_B, \mu_S),$$

$$\rho_B^{\text{mic}} = \frac{1}{V} \sum_i B_i \cdot N_i^{\text{SM}}(T, \mu_B, \mu_S),$$

$$\rho_S^{\text{mic}} = \frac{1}{V} \sum_i S_i \cdot N_i^{\text{SM}}(T, \mu_B, \mu_S).$$

Multiplicity \rightarrow

Energy \rightarrow

Pressure \rightarrow

Entropy density \rightarrow

$$N_i^{\text{SM}} = \frac{V g_i}{2\pi^2 \hbar^3} \int_0^\infty p^2 f(p, m_i) dp,$$

$$E_i^{\text{SM}} = \frac{V g_i}{2\pi^2 \hbar^3} \int_0^\infty p^2 \sqrt{p^2 + m_i^2} f(p, m_i) dp$$

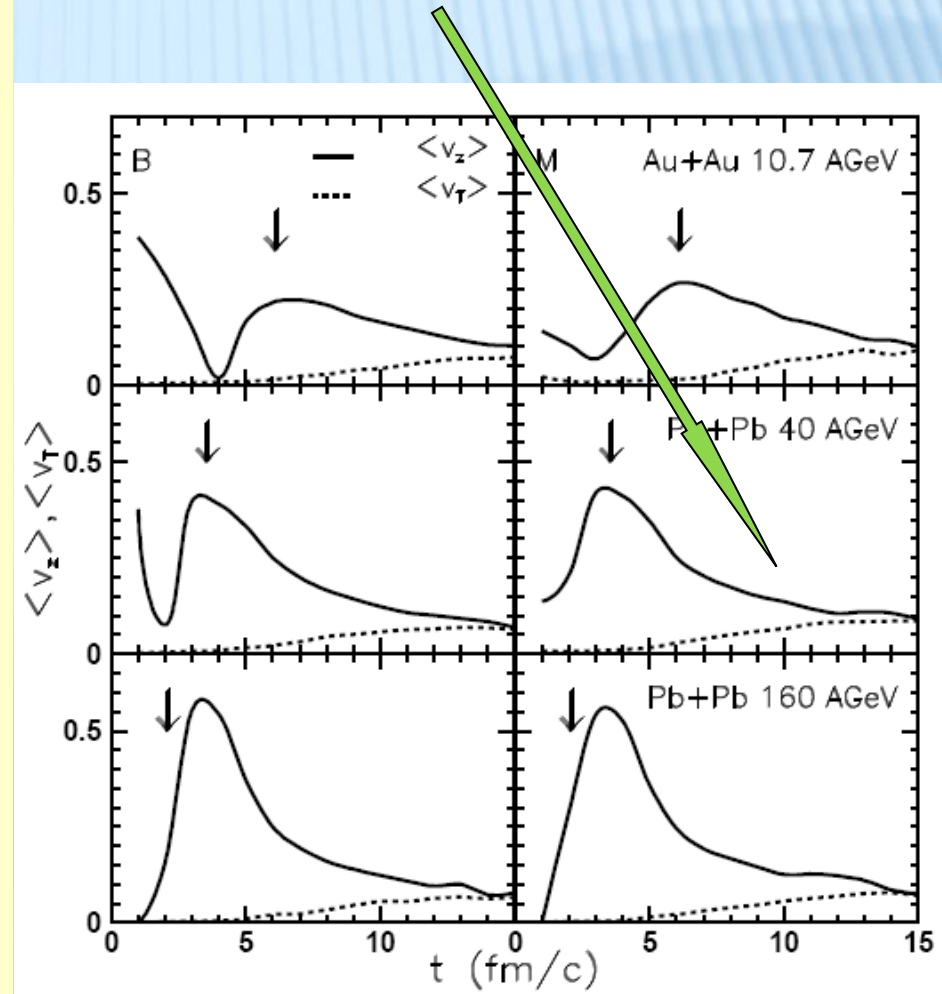
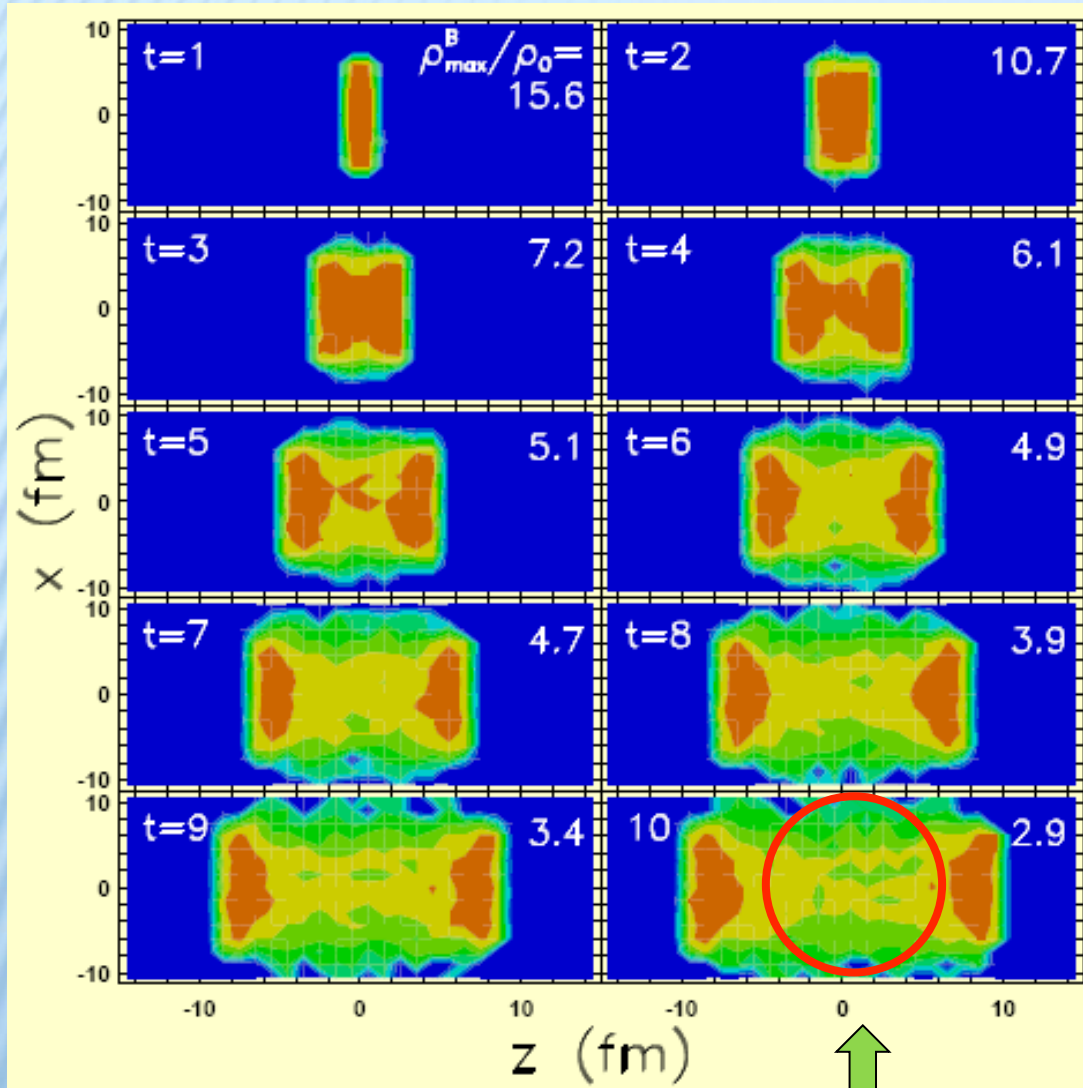
$$P^{\text{SM}} = \sum_i \frac{g_i}{2\pi^2 \hbar^3} \int_0^\infty p^2 \frac{p^2}{3(p^2 + m_i^2)^{1/2}} f(p, m_i) dp$$

$$s^{\text{SM}} = - \sum_i \frac{g_i}{2\pi^2 \hbar^3} \int_0^\infty f(p, m_i) [\ln f(p, m_i) - 1] p^2 dp$$

PRE-EQUILIBRIUM STAGE

Homogeneity of baryon matter

Absence of flow



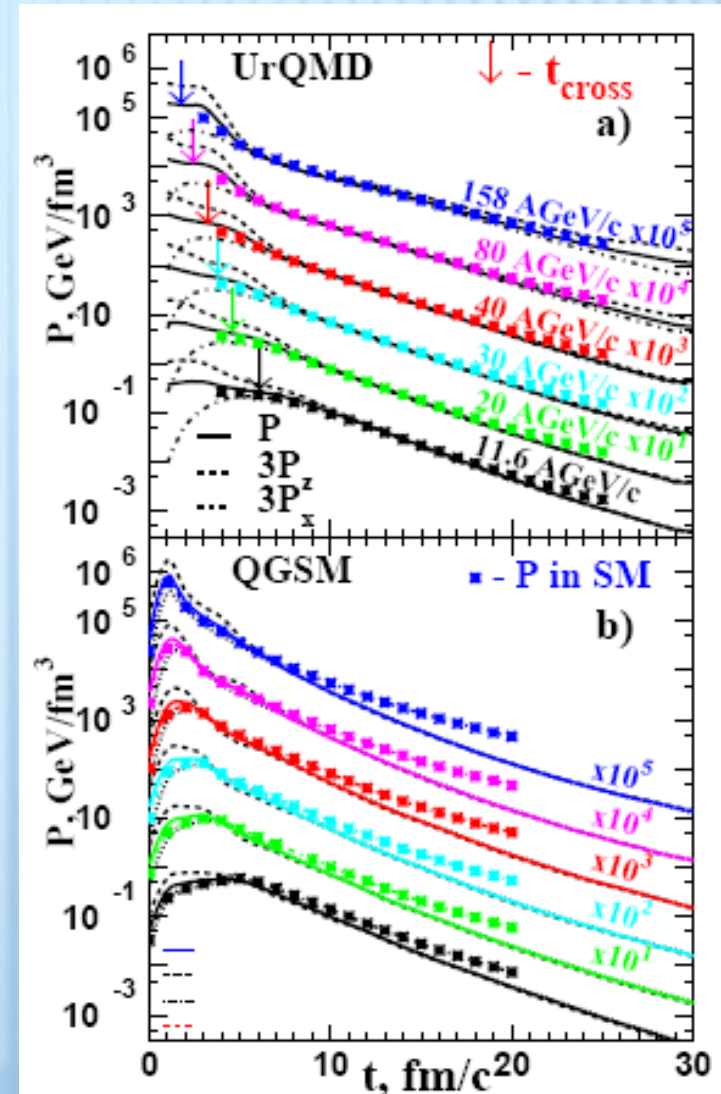
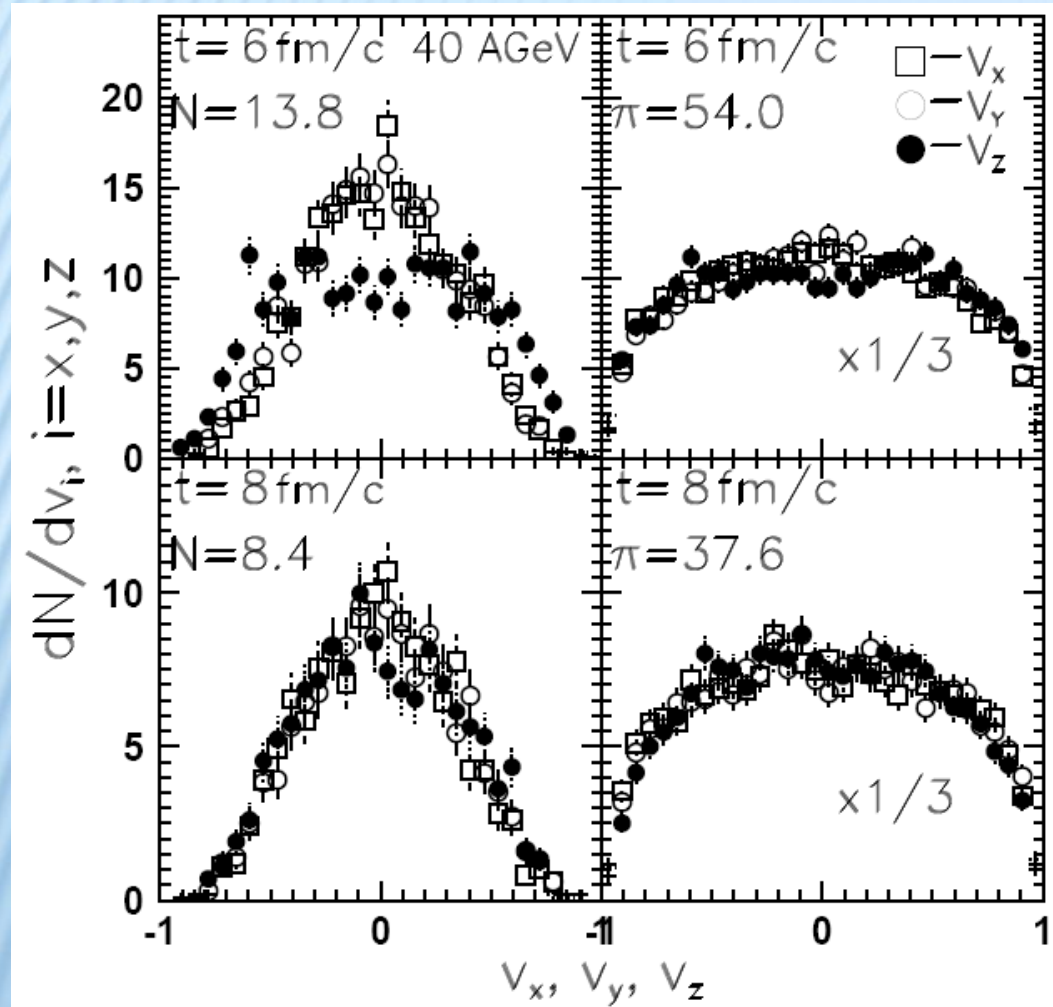
L.Bravina et al., PRC 60 (1999) 024904

The local equilibrium in the central zone is quite possible

KINETIC EQUILIBRIUM

Isotropy of velocity distributions

Isotropy of pressure



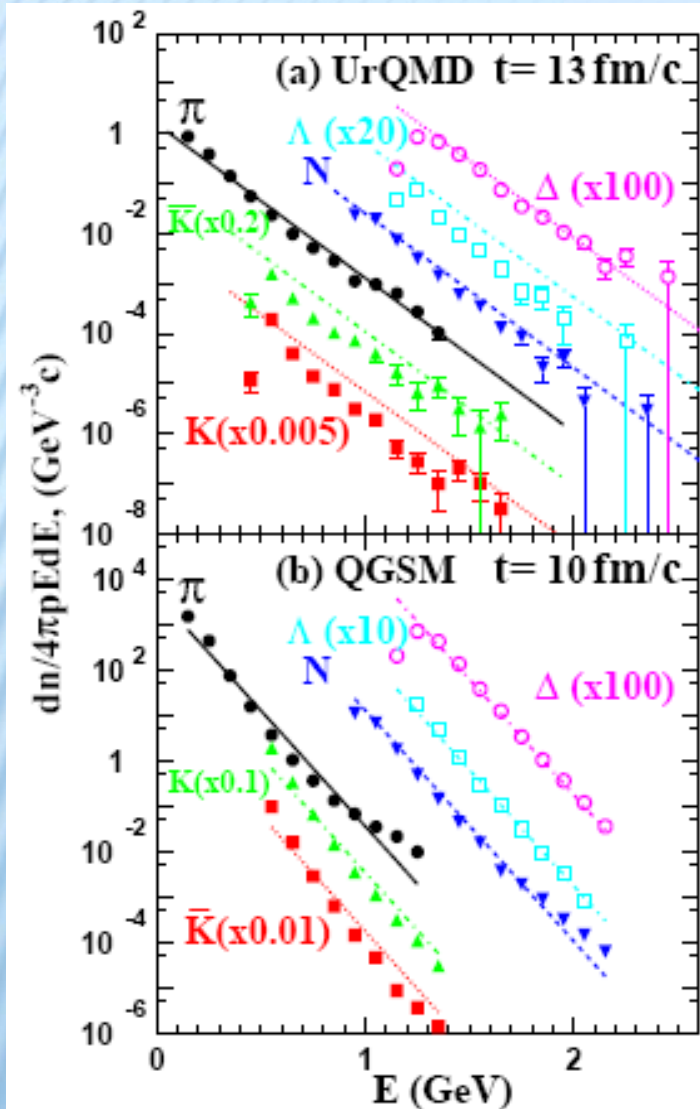
L.Bravina et al., PRC 78 (2008) 014907

Velocity distributions and pressure become isotropic for all energies

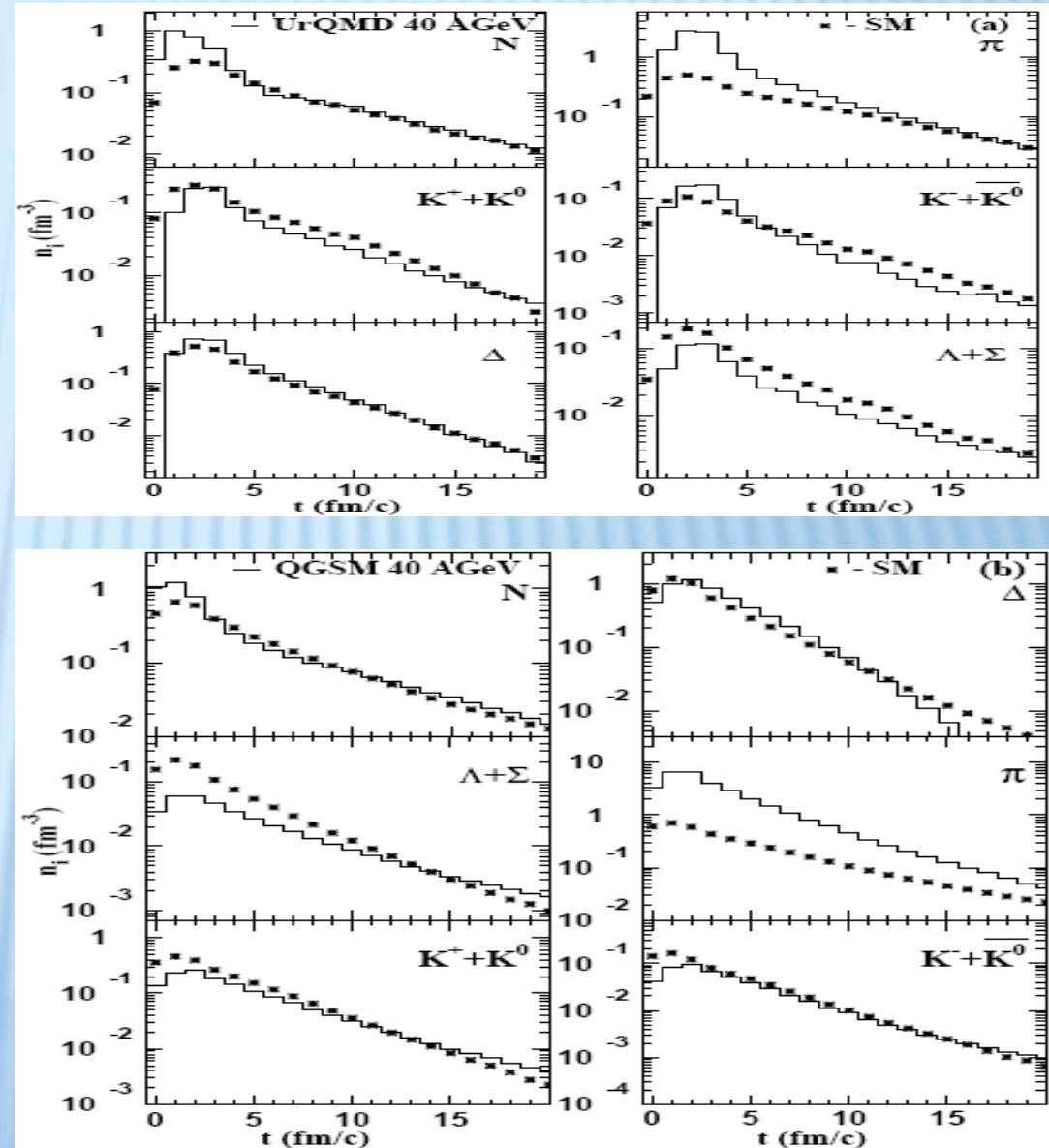
THERMAL AND CHEMICAL EQUILIBRIUM

Boltzmann fit to the energy spectra

Particle yields



L.Bravina et al., PRC 78 (2008) 014907

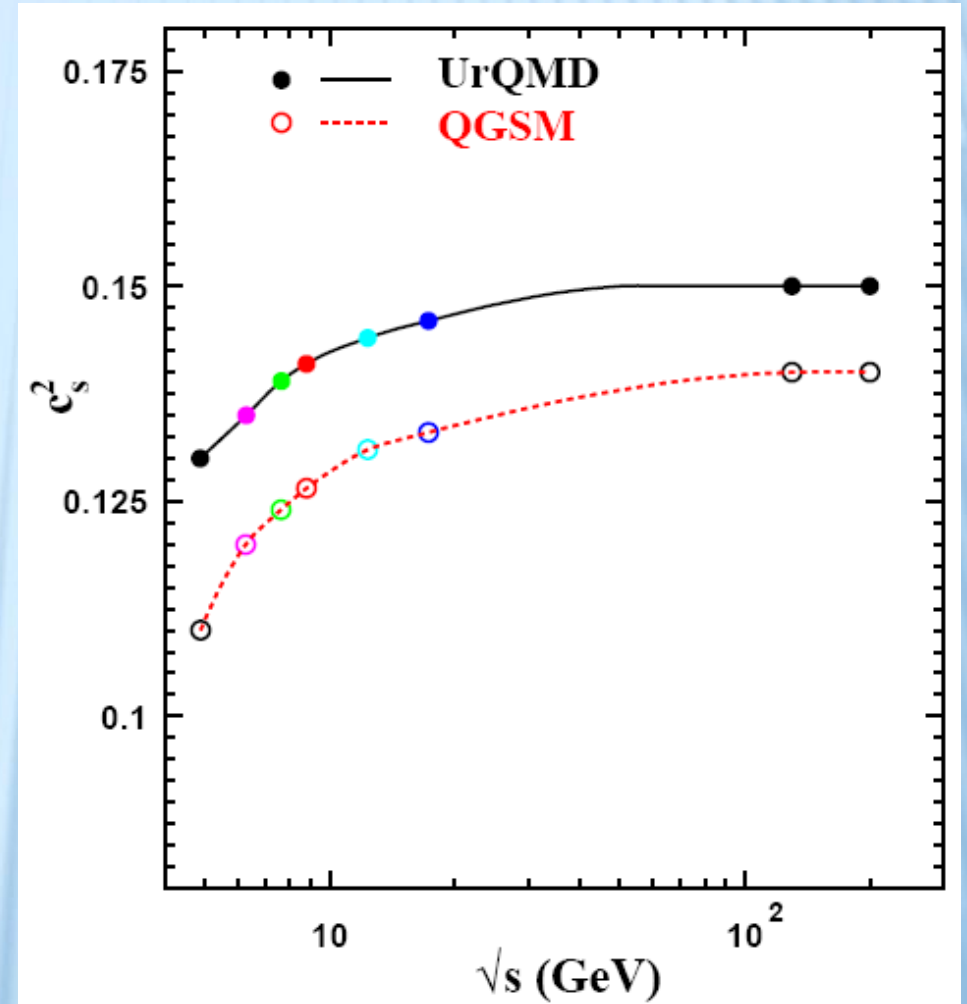
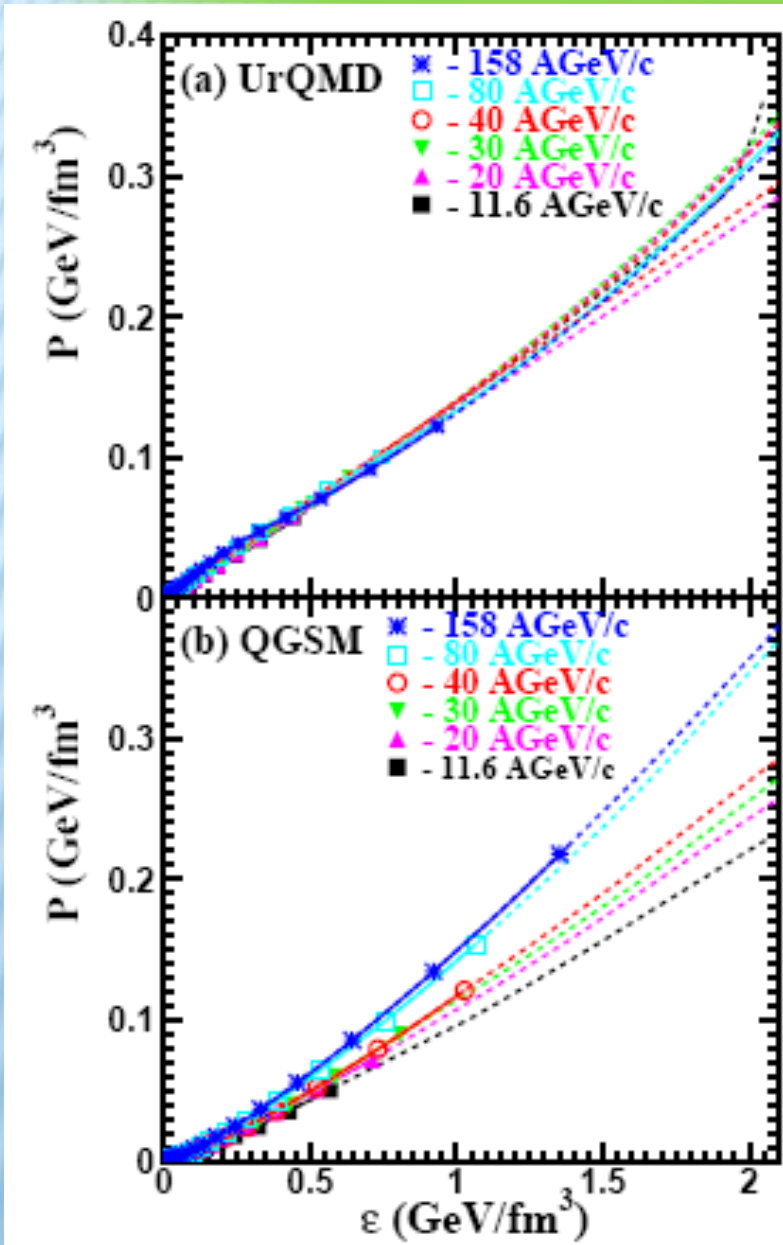


Thermal and chemical equilibrium seems to be reached

EQUATION OF STATE IN THE CELL

pressure vs. energy

sound velocity

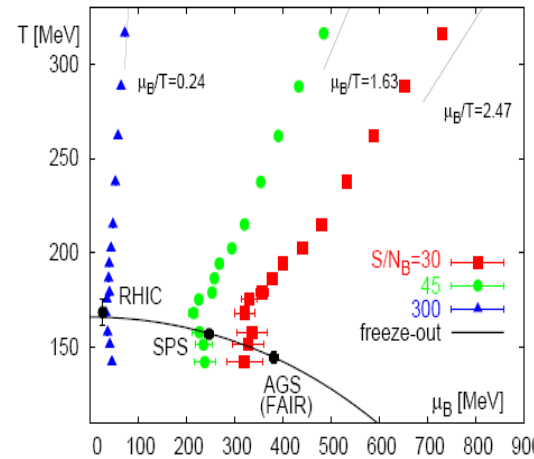


$P/\epsilon = 0.13(\text{AGS}), 0.14(40), 0.146(\text{SPS}), 0.15(\text{RHIC})$

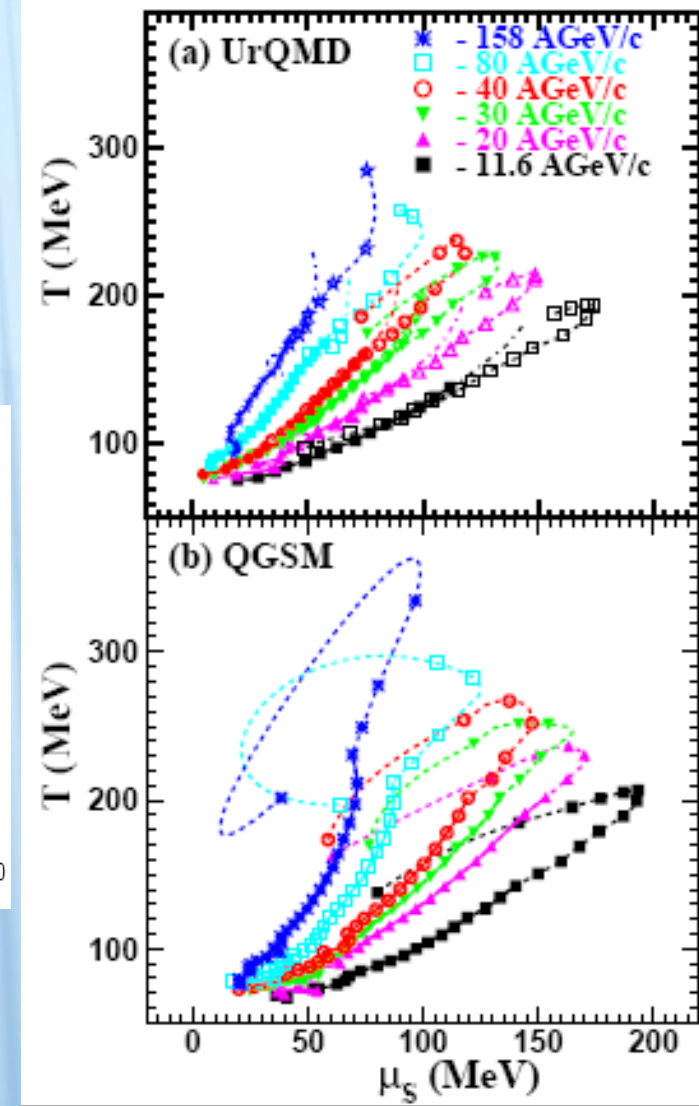
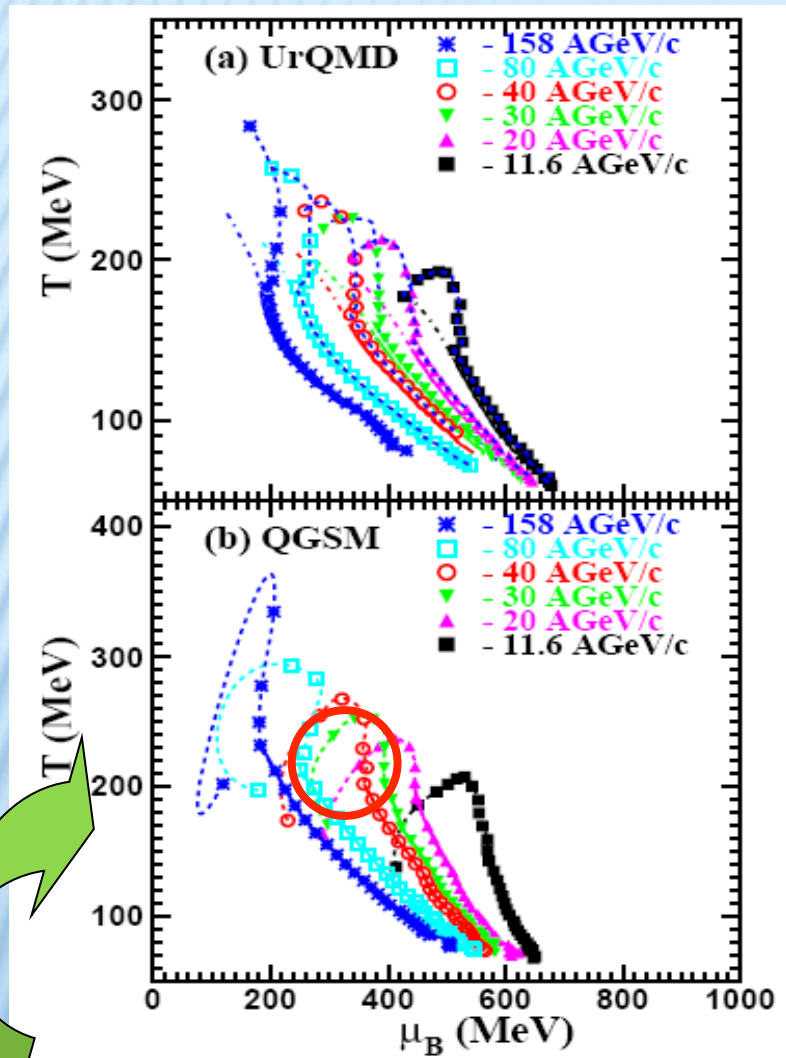
EOS IN THE CELL: OBSERVATION OF KNEE

temperature vs. chemical potentials

L.Bravina et al.,
PRC 78 (2008) 014907



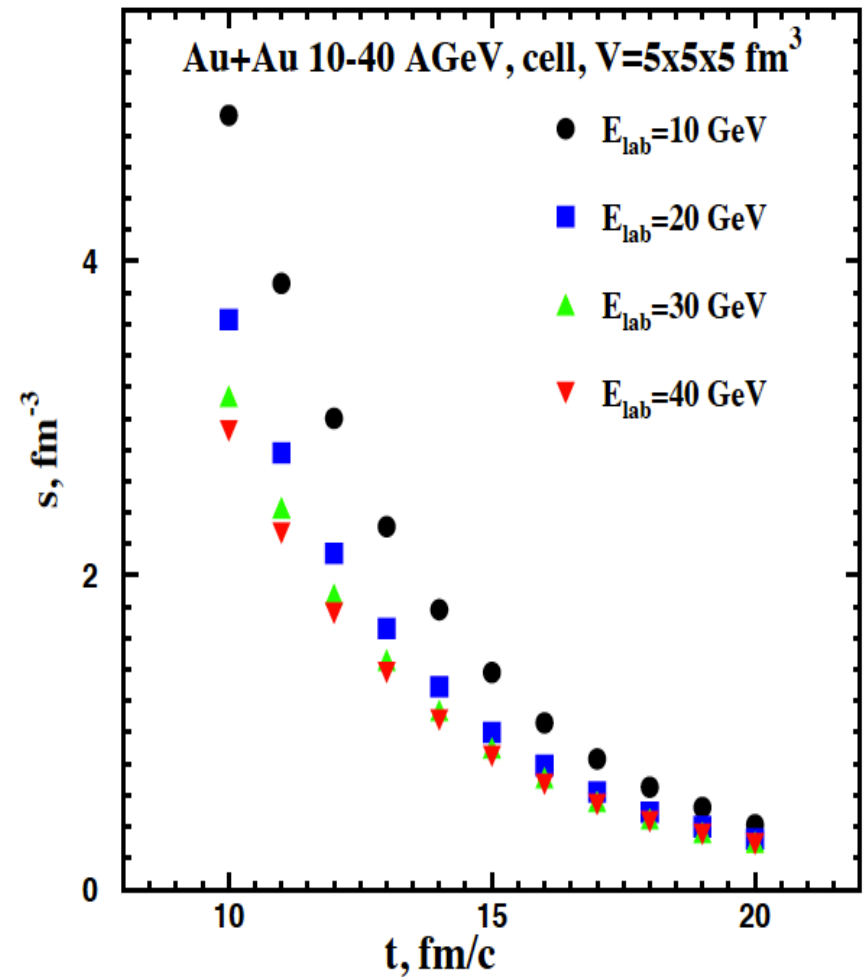
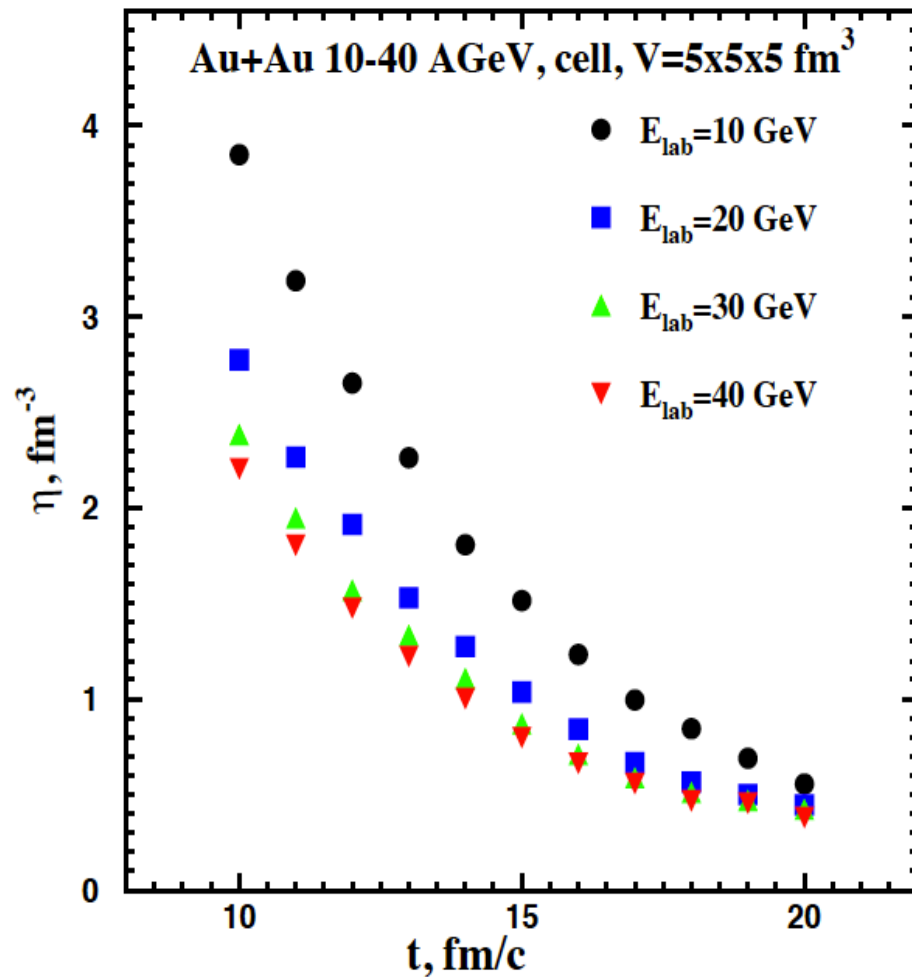
S. Ejiri et al., PRD
73 (2006) 054506



Although the “knee” is similar to that in 2-flavor lattice QCD, it is related to inelastic (chemical) freeze-out in the system

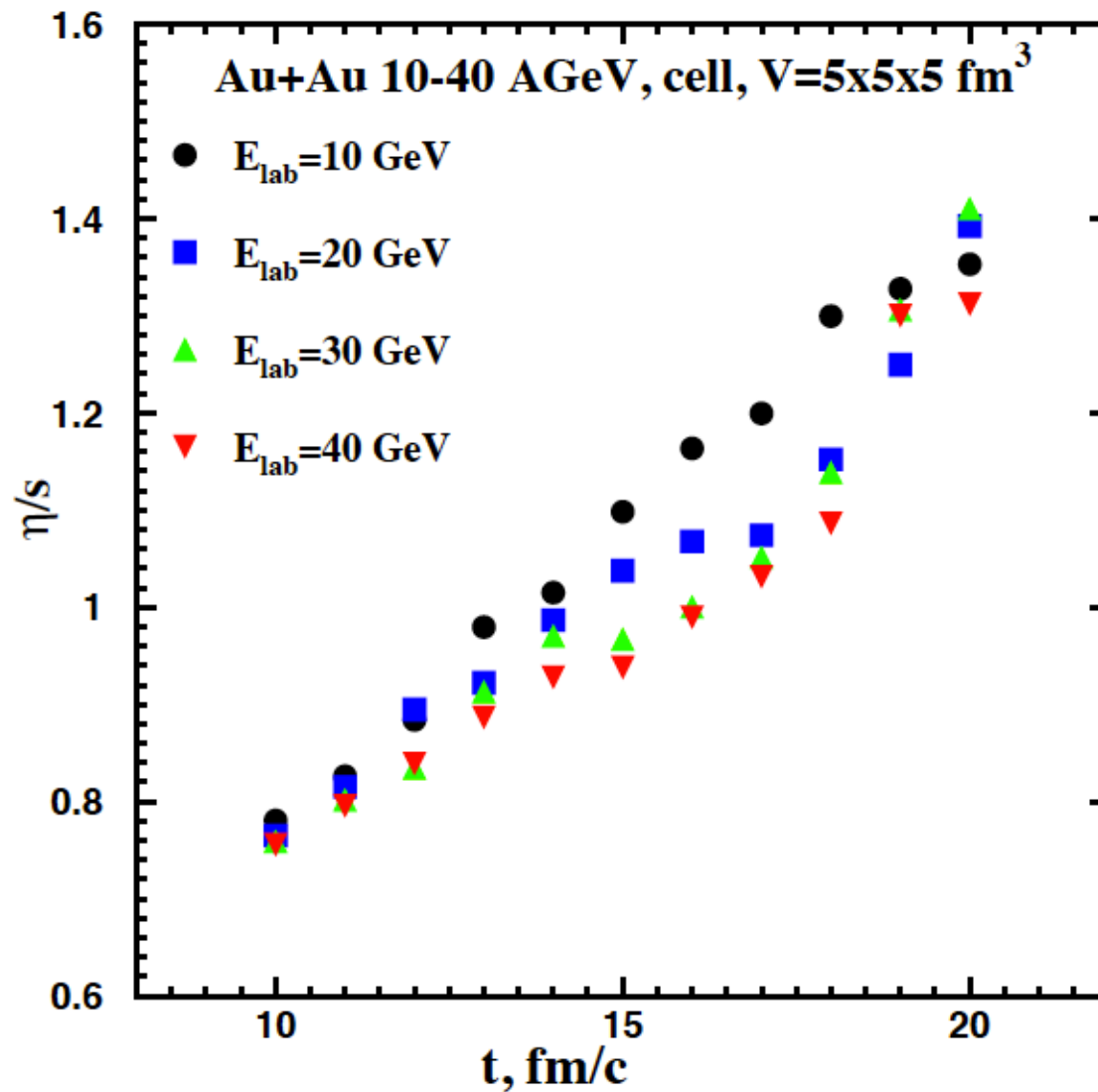
SHEAR VISCOSITY AND ENTROPY

in collaboration with M. Teslyk



SHEAR VISCOSITY AND ENTROPY

in collaboration with M. Teslyk



Conclusions (EOS)

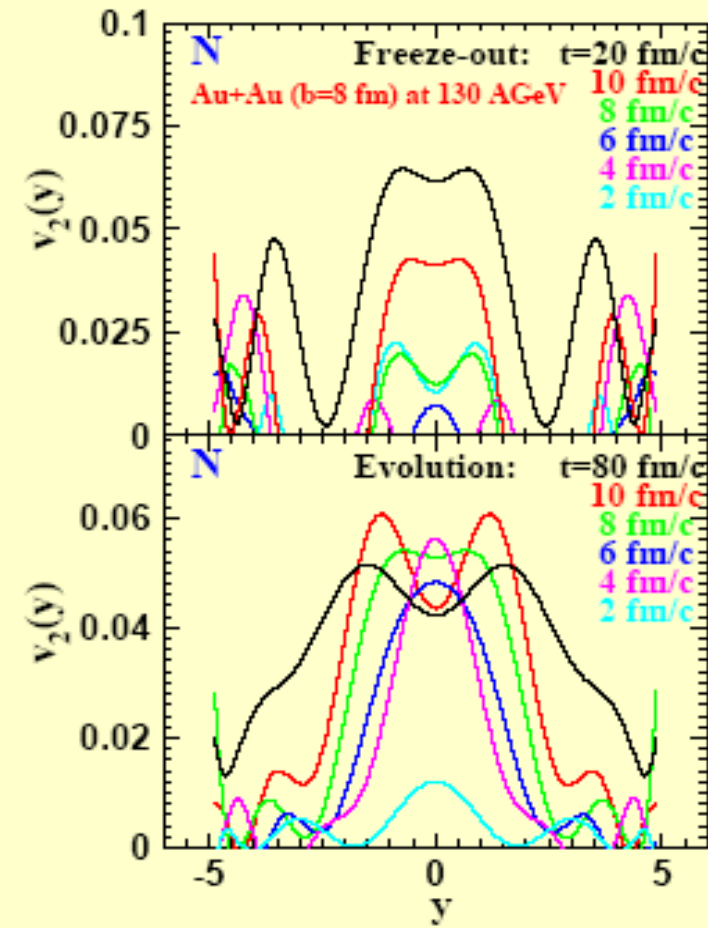
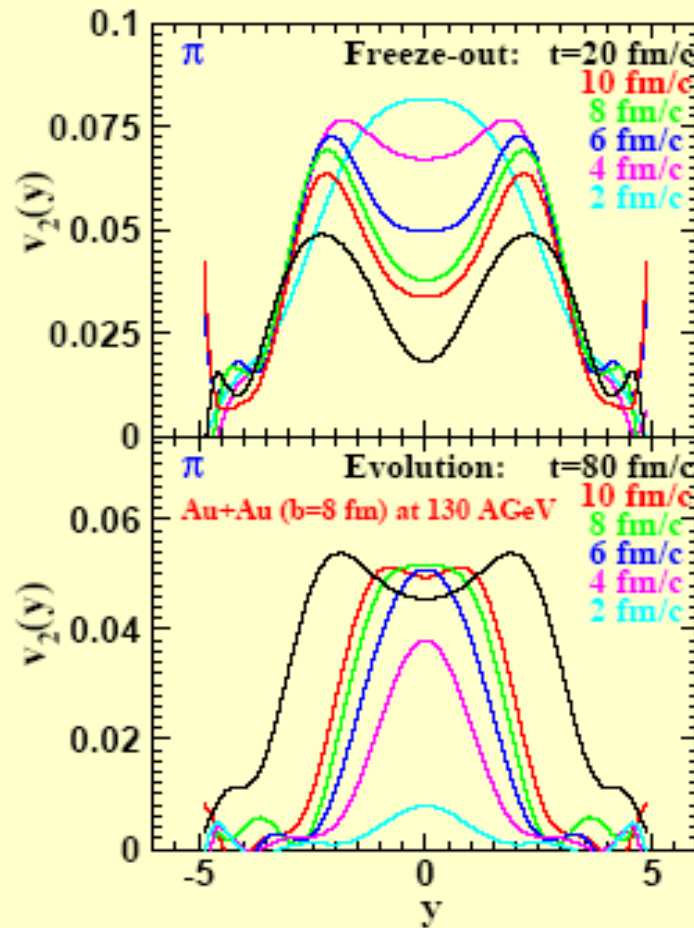
- *Both models favor formation of equilibrated matter for a period of 10-15 fm/c*
- *During this period the expansion of matter in the central cell proceeds isentropically with constant S/B*
- *The EOS has a simple form: $P/e = \text{const}$, where the speed of sound squared varies from 0.12 (AGS) to 0.14 (40 AGeV), and to 0.15 (SPS & RHIC) \Rightarrow onset of saturation*
- *T vs. μ : the knee structure which appears at the onset of equilibrium is related to chemical freeze-out*

Backup slides

TIME EVOLUTION OF ELLIPTIC FLOW (RHIC)

PIONS (Au+Au, 130 AGeV, b=8 fm)

NUCLEONS



- (1) The **earlier** the freeze-out of **pions**, the stronger their elliptic flow
- (2) The **later** the freeze-out of **nucleons**, the stronger their elliptic flow
- (3) The flow formation is not over e.g. at $t = 6$ fm/c due to continuous freeze-out of particles

MPD detector has the same advantages as ALICE to study femtoscopy:

- It can be promising to make 3D CF analysis using heavier particles: K, p because of more Gaussian shape of SF and less influence of resonances
- Different particle pairs: πK , K^+K^- , πp , $\pi \Lambda$, $\Lambda \Lambda$.. can be studied -- different influence of cascade phase, emission asymmetries..
- Az-sensitive femtoscopy is particularly sensitive to the evolution time (in addition to R_{\perp}) and to the expansion velocity.

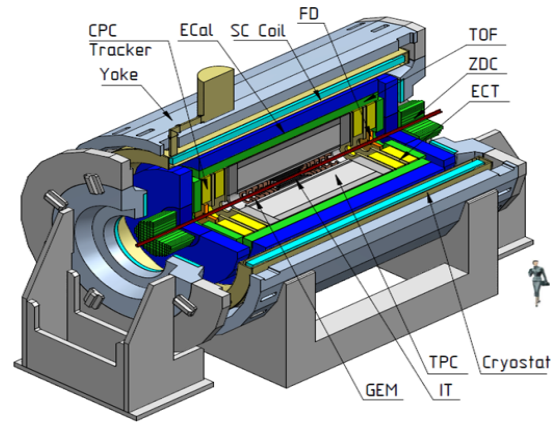
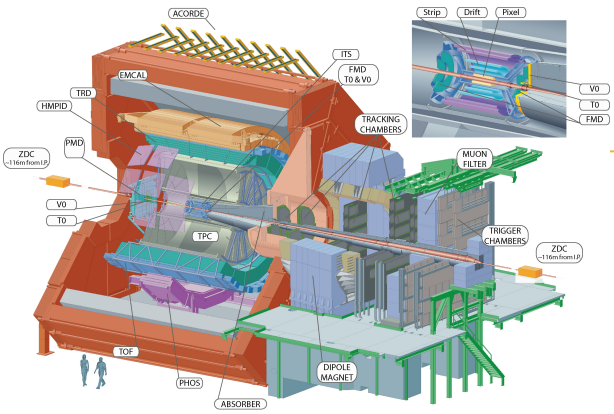
ALICE

- Low momentum cut-off ($p > 100$ MeV/c)
- Small material budget
- Excellent particle identification (PID) by: specific energy loss (dE/dx) & TOF

MPD

- Good primary and secondary vertex resolution

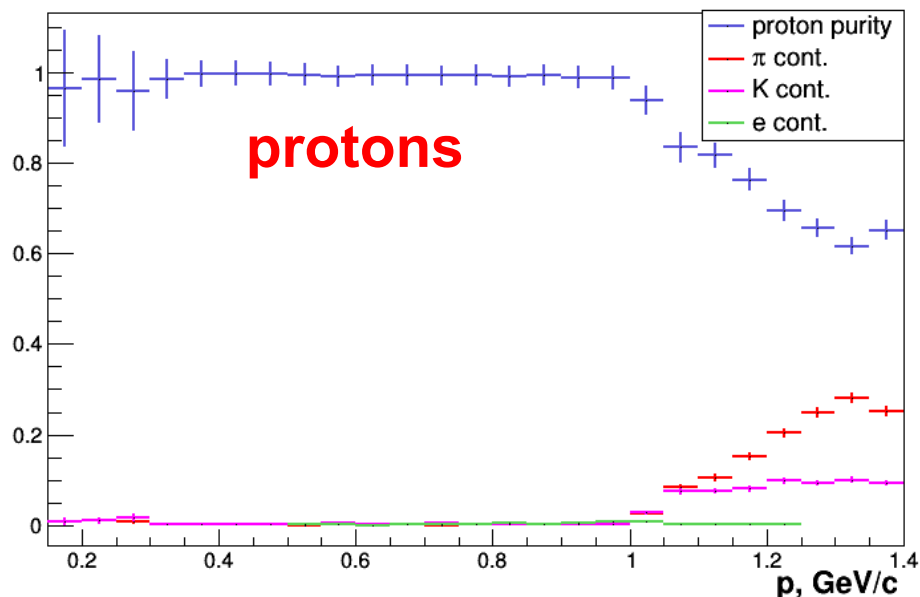
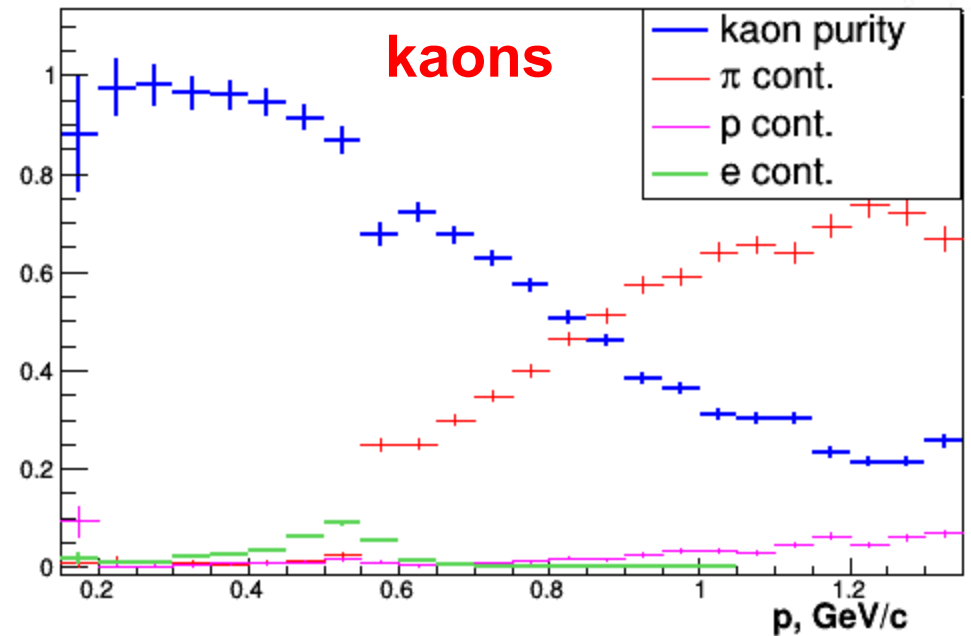
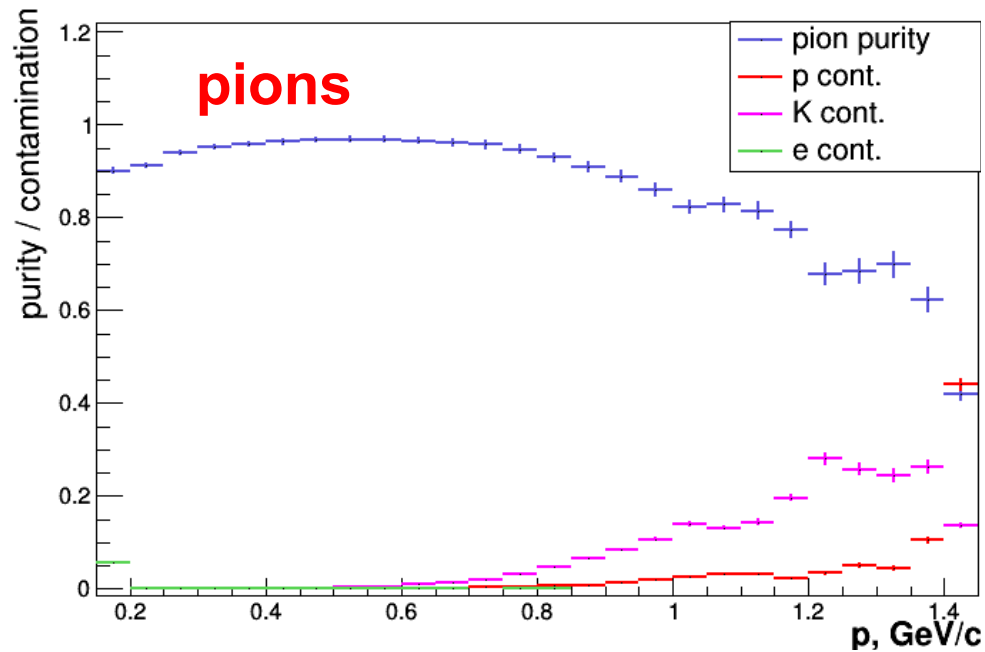
Package for femtoscopy study:
FemtoMPD
 is under development
 ● allows one to estimate influence of the two-track effects (TTE) (splitting & merging) in order to avoid distortion of CF.
PID study is very important



Some results of PID study by MSU group (2017)

- The parameters of dE/dx in TPC BB Aleph parameterization for π , K, p, e were found and stored in the MPD ROOT class.
- The parameters of TOF $1/\beta$ parameterization for π , K, p, e were found and stored in the MPD ROOT class.
- The alternative method of PID : n-sigma method was implemented in MPD ROOT
- Purity and contaminations were estimated for Bayesian method for TPC, TOF, TPC+TOF

Purity / contamination, TPC



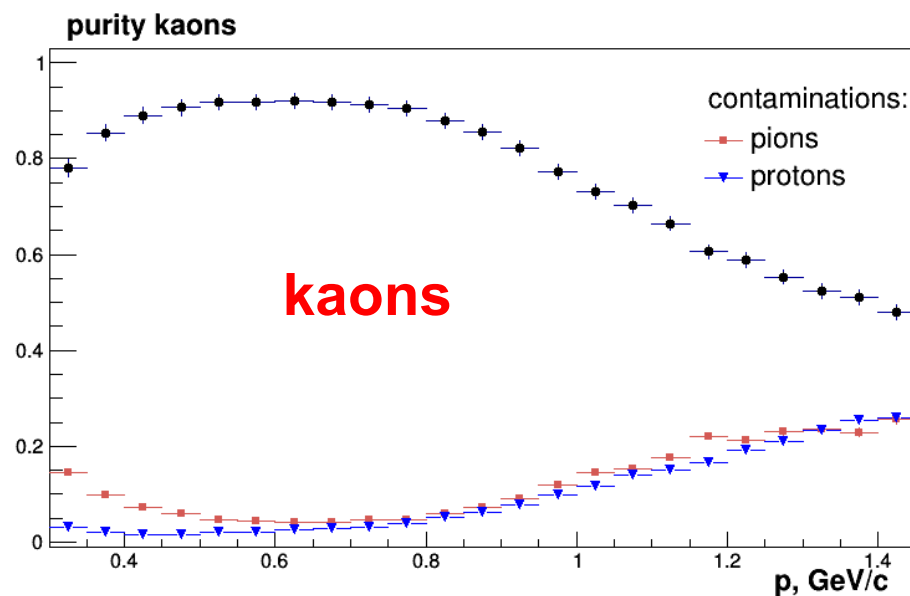
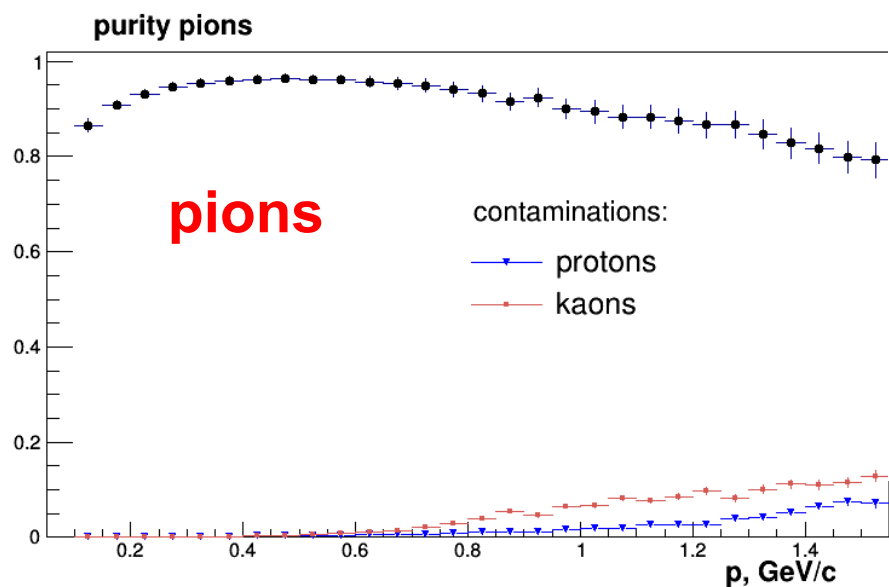
N_i^{meas} : all particles identified as specie I

N_{ii}^{true} : particles identified as specie i, and are actually i (within N_i^{meas})

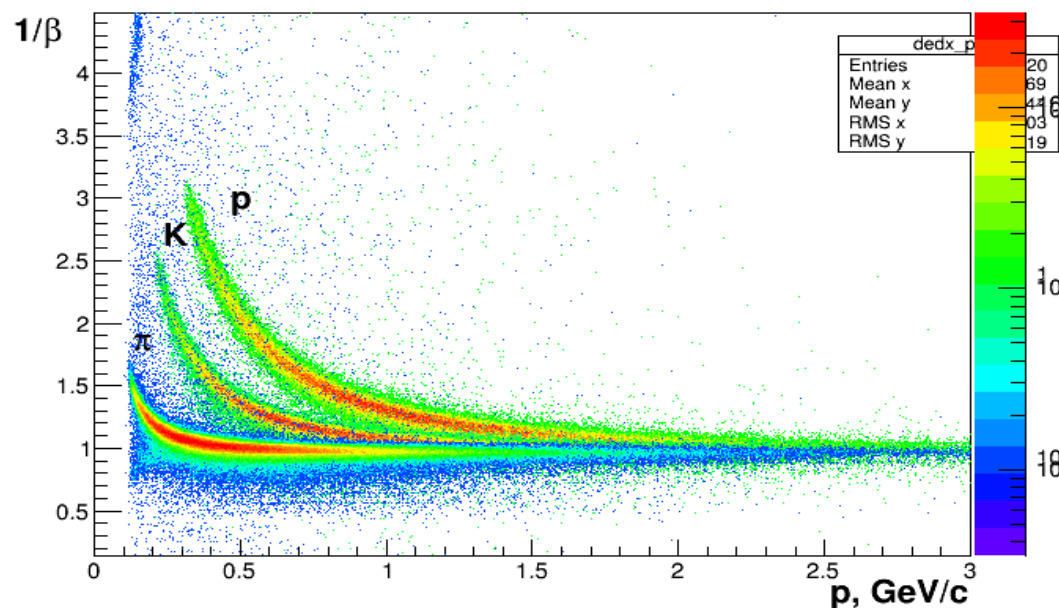
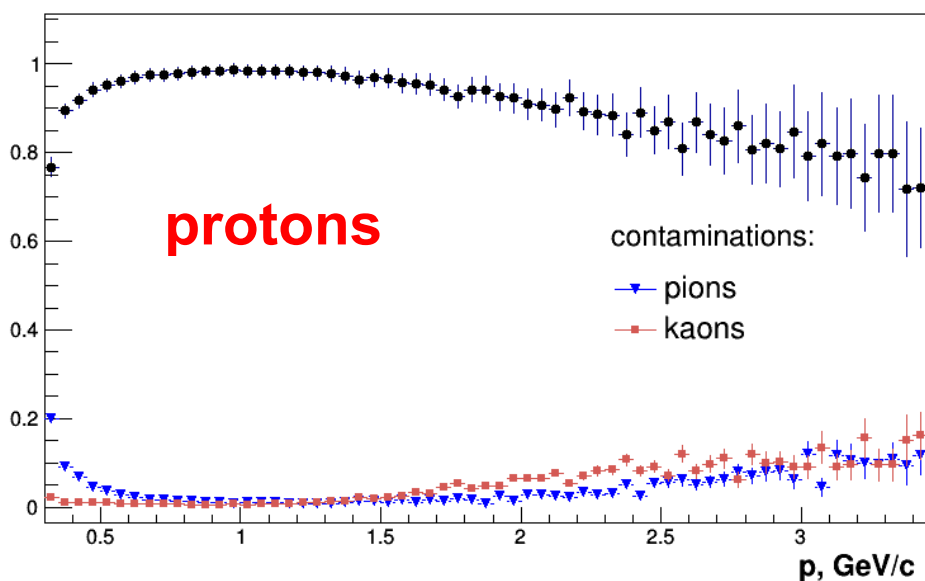
$$\text{Purity} = \frac{N_{ii}^{\text{true}}}{N_i^{\text{meas}}}$$

$$\text{Cont} = \frac{N_{i\bar{i}}^{\text{false measured as i}}}{N_i^{\text{meas}}}$$

Purity / contamination, TOF



purity protons



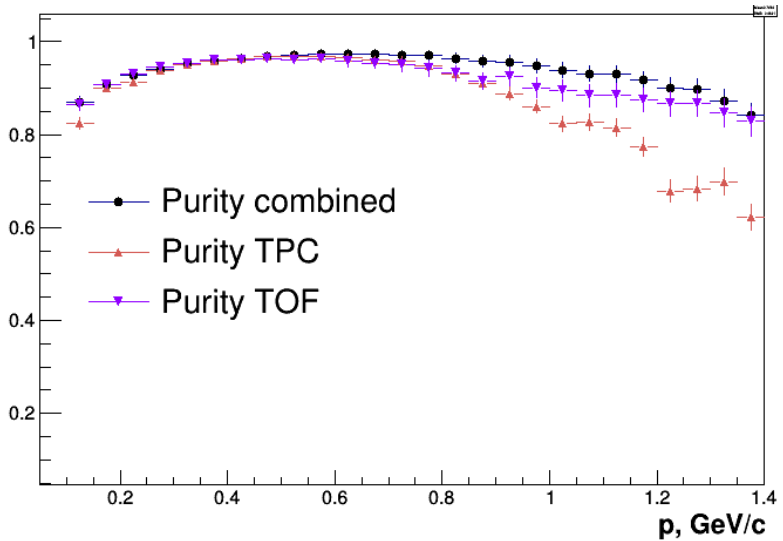
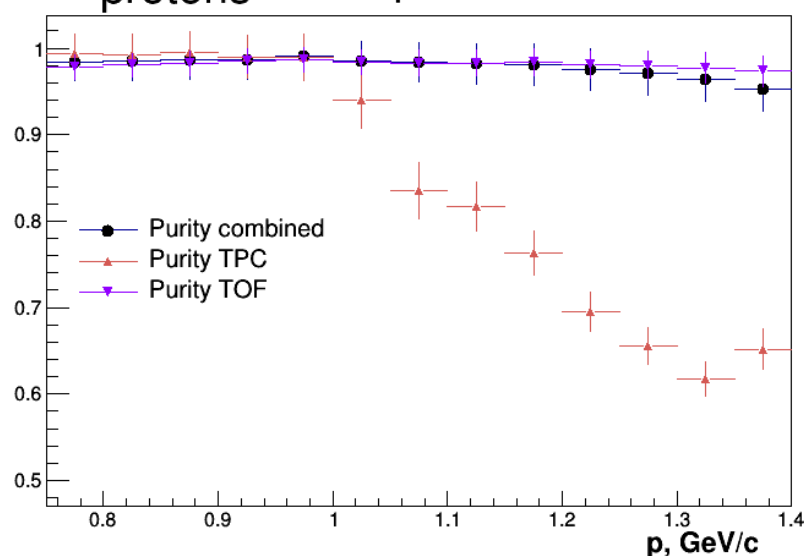
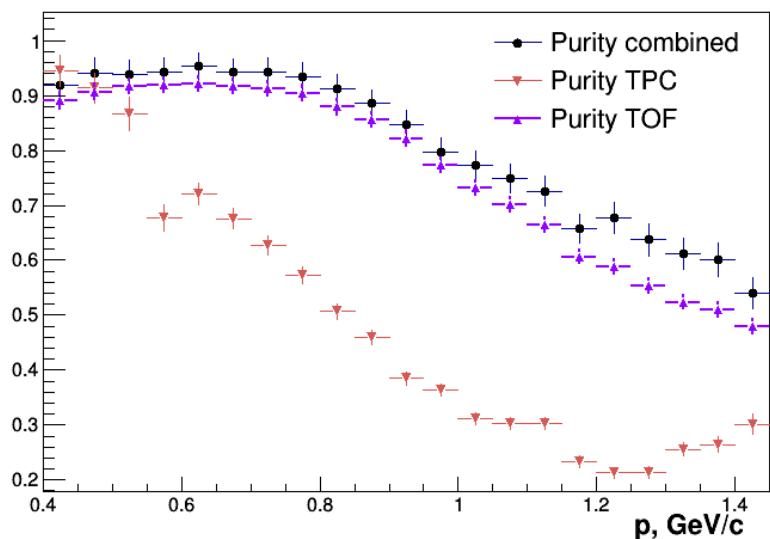
Purity / contamination, TPC +TOF

Combined prob. :

$$P_{i, \text{comb}} = \frac{P_{i, \text{tof}} * P_{i, \text{tpc}}}{\sum P_{i, \text{tof}} * P_{i, \text{tpc}}}$$

$$P_{\text{comb}} = P_{\text{tof}} \text{ if } P_{\text{tpc}} = 0 \text{ (and otherwise)}$$

Kaons



	TPC	TOF	TPC+TOF
π	0.1 < p < 1.3	0.1 < p < 1.8	0.1 < 1.4
K	0.15 < p < 0.7	0.3 < p < 1.4	0.4 < p < 1.5
p	0.1 < p < 1.3	0.4 < p < 3	0.8 < p < 1.4

- Due to acceptance, different p range is used for PID.
 - In a given p range comb. purity is better than a single one.

Bayesian method:

Probability for the particle to be of a type i :

$$P(i) = \frac{1}{\sqrt{2\pi}\sigma_{dE/dx}} \exp\left(-\frac{((dE/dx)_{meas} - (dE/dx)_{BB,i})^2}{2\sigma_{dE/dx}^2}\right)$$

$$w(i) = \frac{C(i)P(i)}{\sum_k P(k)w(k)}, \quad C(i) = \text{a priori probabilities.}$$

For now: $C(i) = 1$.

n-sigma method:

True/false decision for the particle to be of a type i :

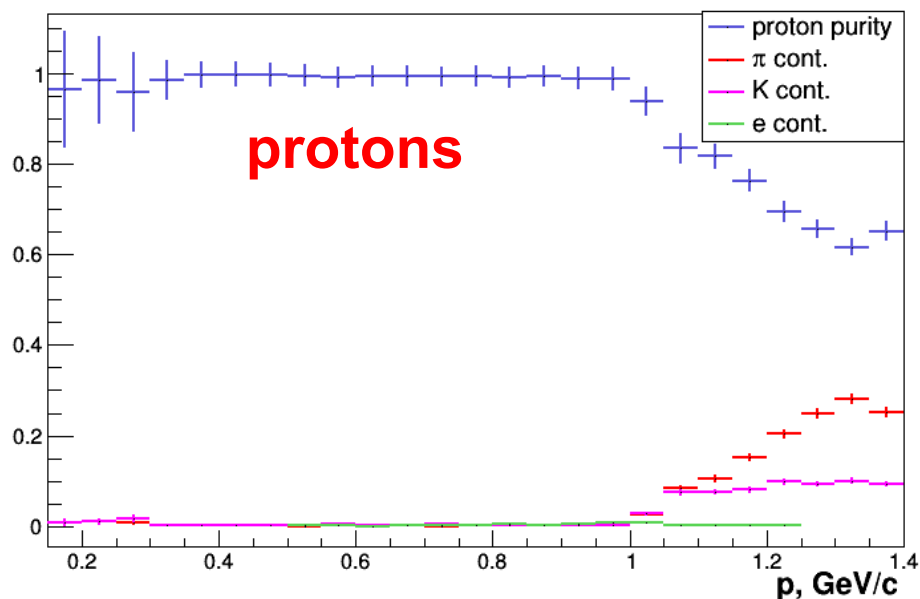
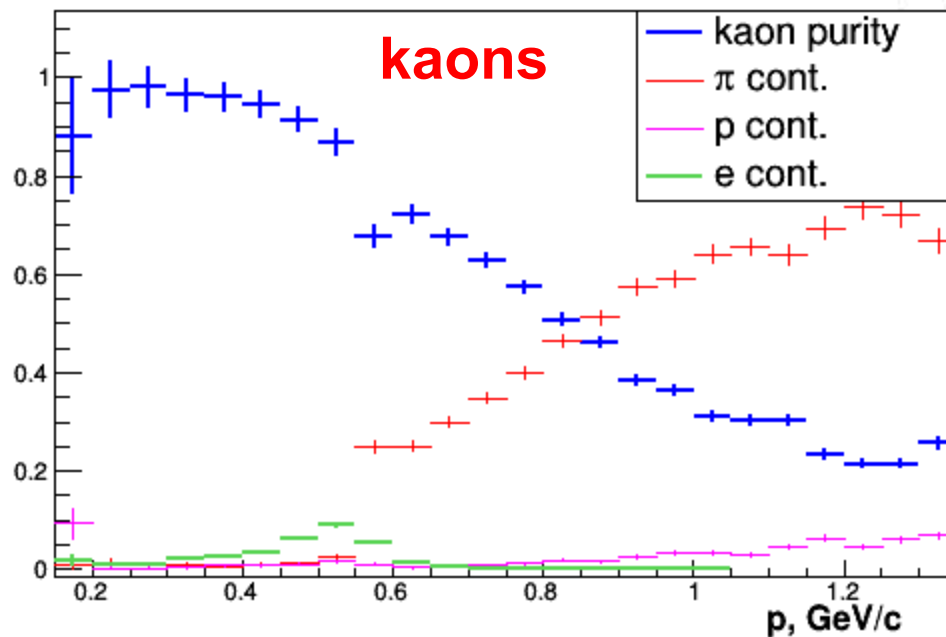
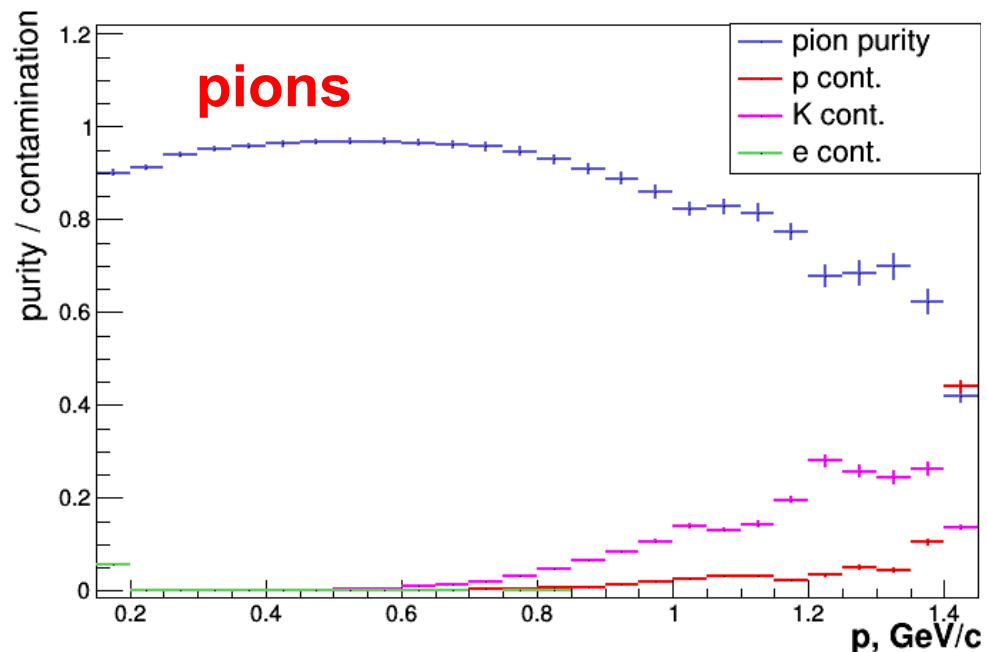
$$\begin{aligned} |(dE/dx)_{meas} - (dE/dx)_{BB,i}| < n^* \sigma_{dE/dx,i} &\rightarrow w(i) = 1 \\ |(dE/dx)_{meas} - (dE/dx)_{BB,i}| > n^* \sigma_{dE/dx,i} &\rightarrow w(i) = 0 \end{aligned}$$

* the n-sigma method because it is more robust and easy to control.

The same for TOF detector: dE/dx (in TPC) $\rightarrow 1/\beta$ (in TOF)

MpdParticleIdentification::SetNSigmaDedx(n) method is added to the class
MpdParticleIdentification::SetNSigmaBeta(n) method is added to the class

Purity / contamination, TPC



N_i^{meas} : all particles identified as specie I

N_{ii}^{true} : particles identified as specie i, and are actually i (within N_i^{meas})

$$\text{Purity} = \frac{N_{\text{true},i}}{N_{\text{mes},i}}$$

$$\text{Cont} = \frac{N_{\text{false measured as } i}}{N_{\text{mes},i}}$$